

We are IntechOpen, the world's leading publisher of Open Access books Built by scientists, for scientists

4,800

Open access books available

122,000

International authors and editors

135M

Downloads

Our authors are among the

154

Countries delivered to

TOP 1%

most cited scientists

12.2%

Contributors from top 500 universities



WEB OF SCIENCE™

Selection of our books indexed in the Book Citation Index
in Web of Science™ Core Collection (BKCI)

Interested in publishing with us?
Contact book.department@intechopen.com

Numbers displayed above are based on latest data collected.
For more information visit www.intechopen.com



COMS, the New Eyes in the Sky for Geostationary Remote Sensing

Han-Dol Kim et al.*

*Korea Aerospace Research Institute (KARI)
Republic of Korea*

1. Introduction

With its successful launch on June 26, 2010, the Communication, Ocean, and Meteorological Satellite (COMS) is currently in the early stage of normal operation for the service to the end users, exhibiting exciting and fruitful performances including the image data from the two on-board optical sensors, Meteorological Imager (MI) and Geostationary Ocean Color Imager (GOCI), and the experimental Ka-band telecommunication. This chapter gives a comprehensive overview of COMS in terms of its key design characteristics, current status of in-orbit performances and its implied role in the geostationary remote sensing, and discusses its potential application and contribution to the world remote sensing community.

2. COMS: Description and overview

COMS is a multi-purpose, multi-mission, geostationary satellite. It has been designed and developed by the joint effort of EADS Astrium and Korea Aerospace Research Institute (KARI), and launched by Ariane 5 ECA L552 V195 of Arianespace on 21:41 (UTC) of June 26 2010. COMS is the first South Korean multi-mission geostationary satellite, and also the first 3-axis stabilized geostationary satellite ever built in Europe for optical remote sensing.

The In Orbit Testing (IOT) of COMS was completed early part of 2011, and since then the satellite has been being successfully operated by KARI for the benefits of all 3 end users: the Korean Meteorological Administration (KMA), the Korea Ocean Research & Development Institute (KORDI) and the Electronics & Telecommunications Research Institute (ETRI).

2.1 COMS overview

COMS is a single geostationary satellite fulfilling 3 rather conflicting missions as follows:

- A meteorological mission by MI

* Gm-Sil Kang¹, Do-Kyung Lee¹, Kyoung-Wook Jin¹, Seok-Bae Seo¹, Hyun-Jong Oh², Joo-Hyung Ryu³, Herve Lambert⁴, Ivan Laine⁴, Philippe Meyer⁴, Pierre Coste⁴ And Jean-Louis Duquesne⁴

¹Korea Aerospace Research Institute (KARI), Republic of Korea

²Korea Meteorological Administration (KMA), Republic of Korea

³Korea Ocean Research & Development Institute (KORDI), Republic of Korea

⁴EADS Astrium, France

- An ocean imager mission by GOCI
- An experimental Ka band telecommunication mission

MI is the common imager with the flight heritage from the later series of GOES and MTSAT satellites, and GOCI is the world's 1st ocean color imager to be operated in the geostationary orbit which has been newly developed for the COMS mission. The spacecraft launch mass is 2460 kg and the size is 2.6 m x 1.8 m x 2.8 m in stowed configuration. The orbital location is 128.2°E, mission lifetime is 7.7 years and design lifetime is 10 years.

Fig. 1 shows COMS both in stowed and deployed configurations, where the MI and GOCI optical instruments located on the earth looking satellite floor can be found with both MODCS (Meteorology and Ocean Data Communication System) antenna and the two small telecommunication Ka band reflectors, along with the COMS flight model during AIT.



Fig. 1. COMS, in stowed and deployed configurations and the flight model during the final stage of AIT (Assembly, Integration and Test) at KARI

The following subsections give a succinct description of COMS system, in terms of its key design characteristics and its unique and salient features on the platform, with a little touch on its development history and with a certain emphasized details on GOCI, along with a brief description on the ground segment.

2.2 Description of COMS system

The COMS system consists of the space segment, which is made up of a COMS spacecraft bus with the three payloads, and the various systems of the ground segment, as depicted in the Fig. 2.

Images captured by MI and GOCI are first interleaved on board and downloaded in L band. Data are separated on ground; MI data are processed (radiometrically calibrated and geometrically corrected) and uploaded again in S-band to the satellite in two formats, LRIT (Low Rate Information Transmission) and HRIT (High Rate Information Transmission). These two new streams of data are again interleaved with the raw data and downloaded in L-band to end users by the satellite which acts as a specific data relay.

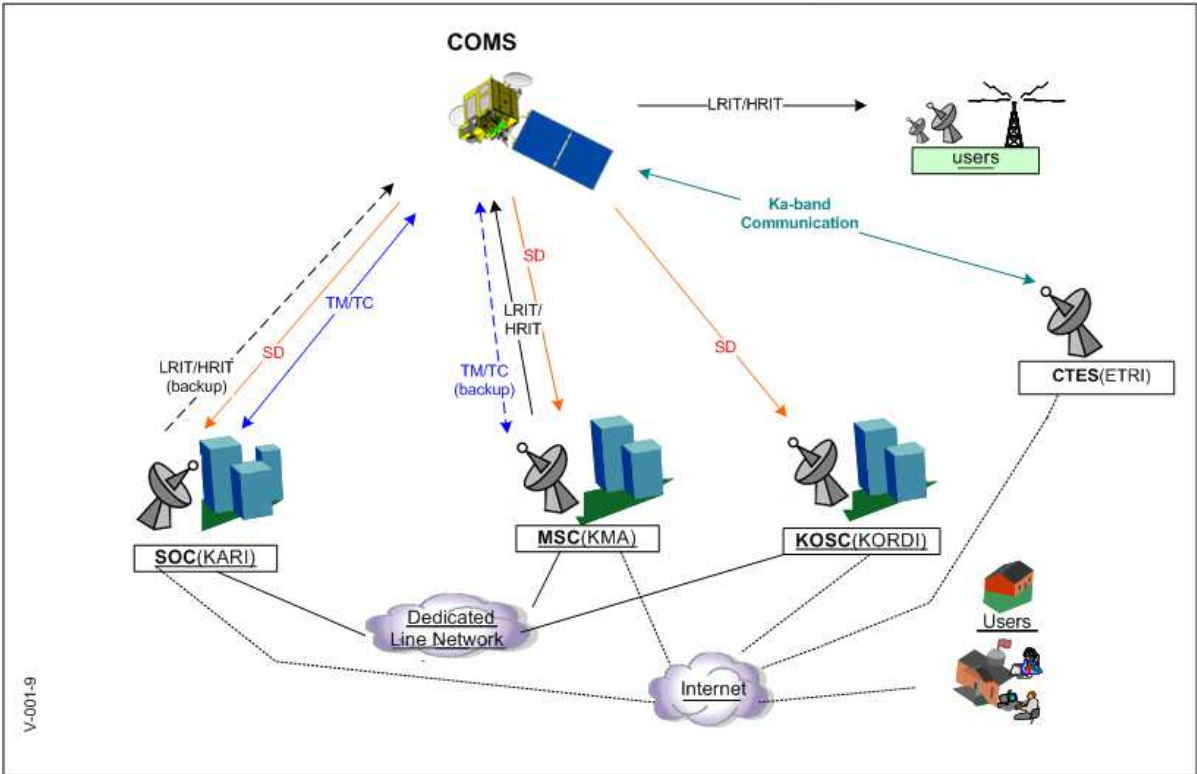


Fig. 2. COMS system overview

2.2.1 COMS spacecraft bus

The COMS spacecraft bus is based on EADS Astrium’s Eurostar-3000 bus design. The satellite features a box-shaped structure, built around the two bi-propellant tanks. Imaging instruments and MODCS antennae are located on the Earth floor (Fig. 1). A single-winged solar array with 10.6 m² of GaAs cells is implemented on the south side, so as to keep the north wall in full view of cold space for the MI radiant cooler. The deployable Ka-band antenna reflectors are accommodated on the east and west walls.

The COMS spacecraft is 3-axis stabilized. Attitude sensing in normal mode is based on a hybridized Earth sensors (IRESs; Infra-Red Earth Sensors) and gyros (FOGs; Fiber Optic Gyros) concept; in addition, sun sensors are being used during 3-axis transfer operations. 5 reaction wheels (RDRs) and 7 thrusters (10 N) serve as actuators. Thrusters are also used for

wheel off-loading and for orbit control. The apogee firing boosts are provided by a 440 N liquid apogee engine.

The key feature of COMS AOCS (Attitude and Orbit Control Subsystem) is the addition of EADS Astrium’s newly developed FOGs, Astrix 120 HR. The FOG allowed the requested performance boost in terms of pointing knowledge and stability to already excellent Eurostar-3000 AOCS design and its performances.

The EPS (Electric Power Subsystem) makes use of GaAs solar cells and Li-ion batteries. A regulated power bus (50 V) distributes power to the various onboard applications through the power shunt regulator. During orbital eclipses, energy is provided by a 154 Ah Li-ion battery. The power at EOL (End Of Life) shall be greater than 2.5 KW.

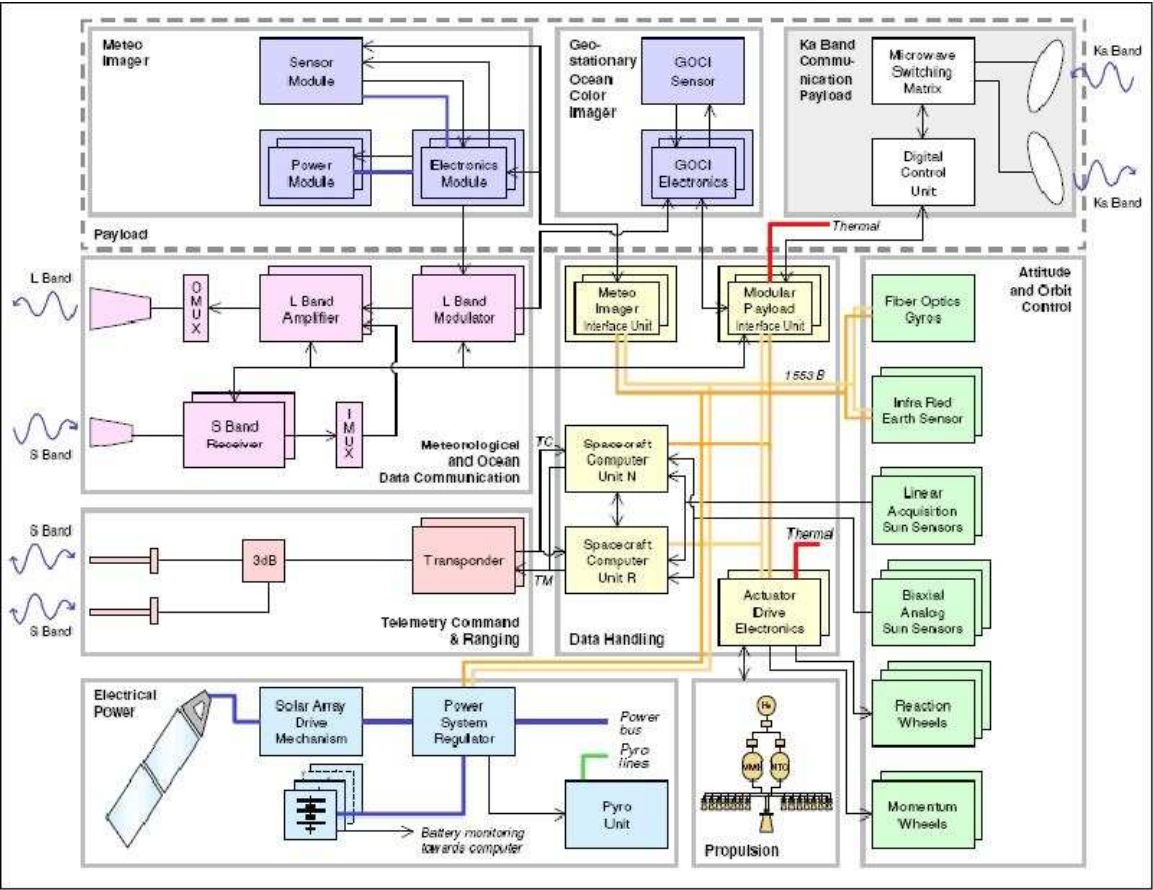


Fig. 3. Block diagram of COMS spacecraft functional architecture

The heart of the avionics architecture is implemented in hot redundant spacecraft computer units, based on 1750 standard processors with Ada object-oriented real-time software. A redundant MIL-STD-1553-B data bus serves as the main data path between the onboard units. Interface units are being used for the serial links, namely the actuator drive electronics with the bus units (including thermal control), the modular payload interface unit with the Ka-band communication payload, and the MI interface unit with the MI instrument.

A specific module (MODCS; Meteorology and Ocean Data Communication System) was developed for handling MI and GOCI images. It collects and transmits raw MI and GOCI data in L-band. HRIT/LRIT (High- and Low-Rate Information Transmission) formats are

generated on the ground from the MI raw data, and uploaded to the satellite in S-Band and relayed in L-band to MI end users.

S-band is also used for satellite Telemetry and Telecommands.

2.2.2 MI

MI is a two-axis scan imaging radiometer from ITT. It senses basically the radiant and solar reflected energies from the Earth simultaneously and provides imagery and radiometric information of the Earth’s surface and cloud cover. It features 1 visible (VIS) channel and 4 infra-red (IR) channels as a scanning radiometer. The design of it is derived from the GOES imager for COMS program.

| No. | Channel | Wavelength(μm) | IFOV(μrad) | GSD(Km) | Dynamic Range |
|-----|---------|----------------|------------|---------|---------------|
| 1 | VIS | 0.55~0.80 | 28 | 1 | 0~115% albedo |
| 2 | SWIR | 3.50~4.00 | 112 | 4 | 110K~350K |
| 3 | WV | 6.50~7.00 | 112 | 4 | 110K~330K |
| 4 | WIN1 | 10.3~11.3 | 112 | 4 | 110K~330K |
| 5 | WIN2 | 11.5~12.5 | 112 | 4 | 110K~330K |

Table 1. Spectral channel characteristics of MI as requirement

MI consists of three modules; sensor module, electronics module, and power supply module. The sensor module contains a scan assembly, a telescope and detectors, and is mounted on spacecraft with the shields, louver and cooler for thermal control. The electronics module which has some redundant circuits performs command, control, signal processing and telemetry conditioning function. The power supply module contains power converters, fuses and power control for interfacing with the spacecraft power system with redundancy.

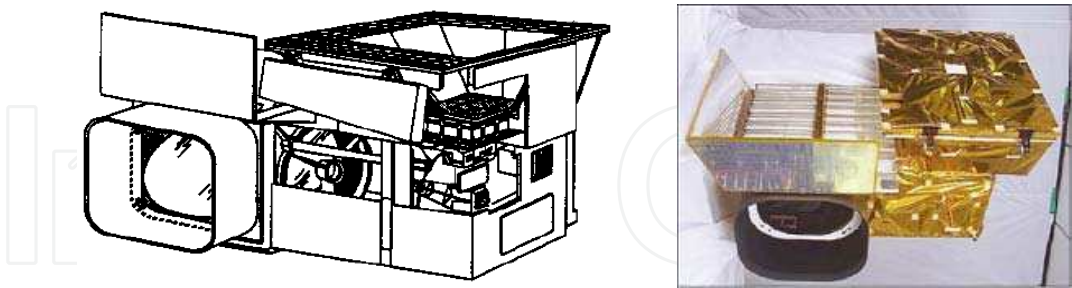


Fig. 4. COMS MI sensor module, in design and flight model configurations

The servo-driven, two-axis gimballed scan mirror of the MI reflects scene energy reflected and emitted from the Earth into the telescope of the MI as shown in the Fig. 5. The mirror scans the Earth with a bi-directional raster scan, which sweeps an 8 km swath along East-West (EW) direction and steps every 8 km along North-South (NS) direction. The area of the observed scene depends on the 2-dimensional angular range of the scan mirror movement. The scene radiance, collected by the scan mirror and the telescope, is separated into each spectral channel by dichroic beam splitters, which allow the geometrically-corresponding detectors of each channel to look at the same position on the Earth. Each detector converts

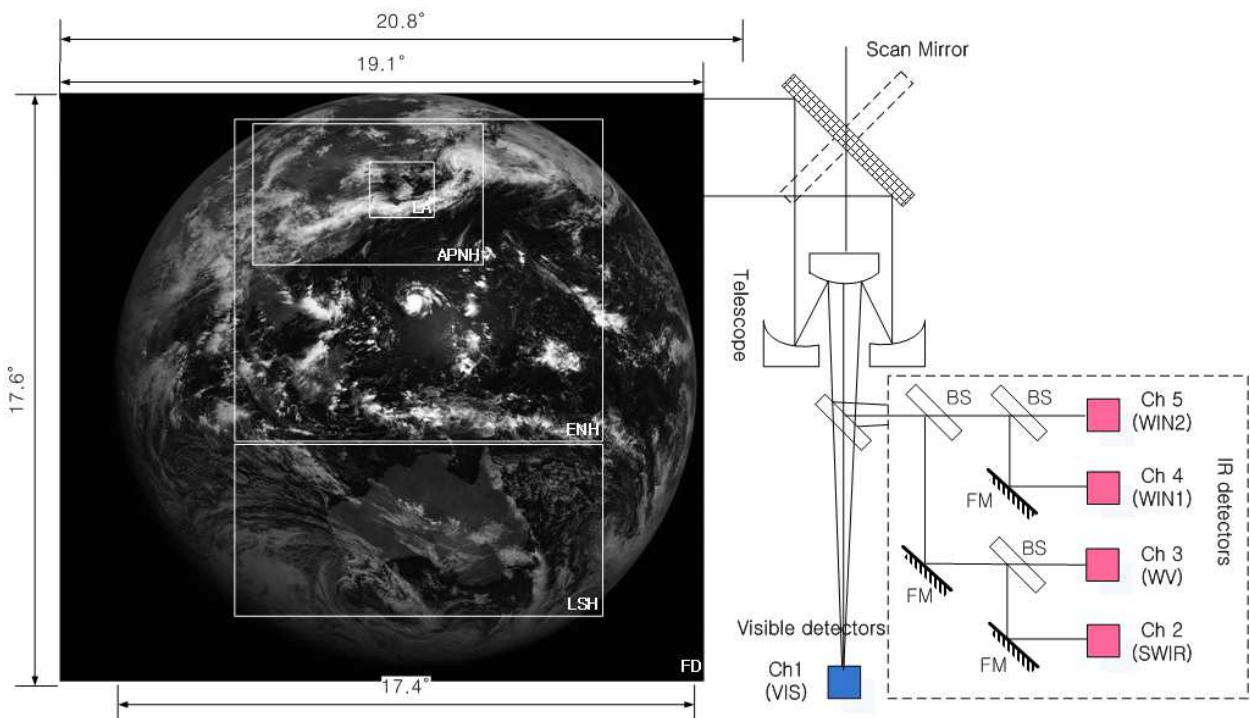


Fig. 5. MI Scan Frame and Schematic design of Optics (BS:Beam Splitter, FM:Folding Mirror, FD: Full Disk, APNH:Asia and Pacific in Northern Hemisphere, ENH:Extended Northern Hemisphere, LSH:Limited Southern Hemisphere, LA: Local Area)

the scene radiance into an electrical signal. The five channel detectors of the MI are divided into two sides, which are electrically redundant each other. Only one side operates at one time by choosing side 1 or side 2 electronics. The visible silicon detector array contains eight detector elements which are active simultaneously in the either side mode. Each visible detector element produces the instantaneous field of view (IFOV) of $28\text{ }\mu\text{rad}$ on a side, which corresponds to 1km on the surface of the Earth at the spacecraft's suborbital point. Each IR channel has two detector elements which are active simultaneously in the either side mode. The SWIR channel employs InSb detectors and the other IR channels use HgCdTe detectors. Each IR detector element produces the IFOV of $112\text{ }\mu\text{rad}$ on a side, which corresponds to 4km on the surface of the Earth at the spacecraft's suborbital point. The 8 visible detector elements and 2 IR detector elements produce the swath width (8 km) of one EW scan line respectively.

The passive radiant cooler with thermostatically controlled heater maintains the infrared detectors at one of the three, command-selectable, cryogenic temperatures. Visible light detectors are at the instrument ambient temperature. Preamplifiers convert low level outputs of all detectors into higher level, low impedance signals as the inputs to the electronics module. MI carries an on-board blackbody target inside of the sensor module for the in-orbit radiometric calibration of the IR channels. The blackbody target is located at the opposite direction to the nadir, so that the scan mirror is rotated 180 degrees in the NS direction from the imaging mode for the blackbody calibration. The full aperture blackbody calibration can be performed by the scan mirror's pointing at the on-board blackbody target via ground command or automatically. The albedo monitor is mounted in the sensor module to measure the in-orbit response change of the visible channel over the mission life.

It uses sunlight through a small aperture as a source. In addition to the radiometric calibration, an electrical calibration is provided to check the stability and the linearity of the output data of the MI signal processing electronics by using an internal reference signal. MI has the star sensing capability in the visible channel, which can be used for image navigation and registration purposes.

MI has three observation modes: global, regional and local modes, which are specialized for the meteorological missions. The global mode is for taking images of the Full Disk (FD) of the Earth. The regional observation mode is for taking images of the Asia and Pacific in North Hemisphere (APNH), the Extended North Hemisphere (ENH), and Limited Southern Hemisphere (LSH). The image of Limited Full Disk (LFD) area can be obtained by the combination of the images of ENH and LSH. The local observation mode is activated for Local Area (LA) coverage in the FD. The user interest of the MI observation areas for FD, APNH, ENH, LSH, LFD, and LA is shown in the Fig. 5.

2.2.3 GOCI

Geostationary Ocean Color Imager (GOCI), the first Ocean Colour Imager to operate from geostationary orbit, is designed to provide multi-spectral data to detect, monitor, quantify, and predict short term changes of coastal ocean environment for marine science research and application purpose. GOCI has been developed to provide a monitoring of Ocean Color around the Korean Peninsula from geostationary platforms in a joint effort by Korea Aerospace Research Institute (KARI) and EADS Astrium under the contract of Communication, Ocean, and Meteorological Satellite (COMS) of Korea.

2.2.3.1 GOCI mission overview

Main mission requirement for GOCI is to provide a multi-spectral ocean image of area around South Korea eight times per day as shown in Fig. 6. The imaging coverage area is 2500x2500 km² and the ground pixel size is 500x500 m² at centre of field, defined at (130°E -

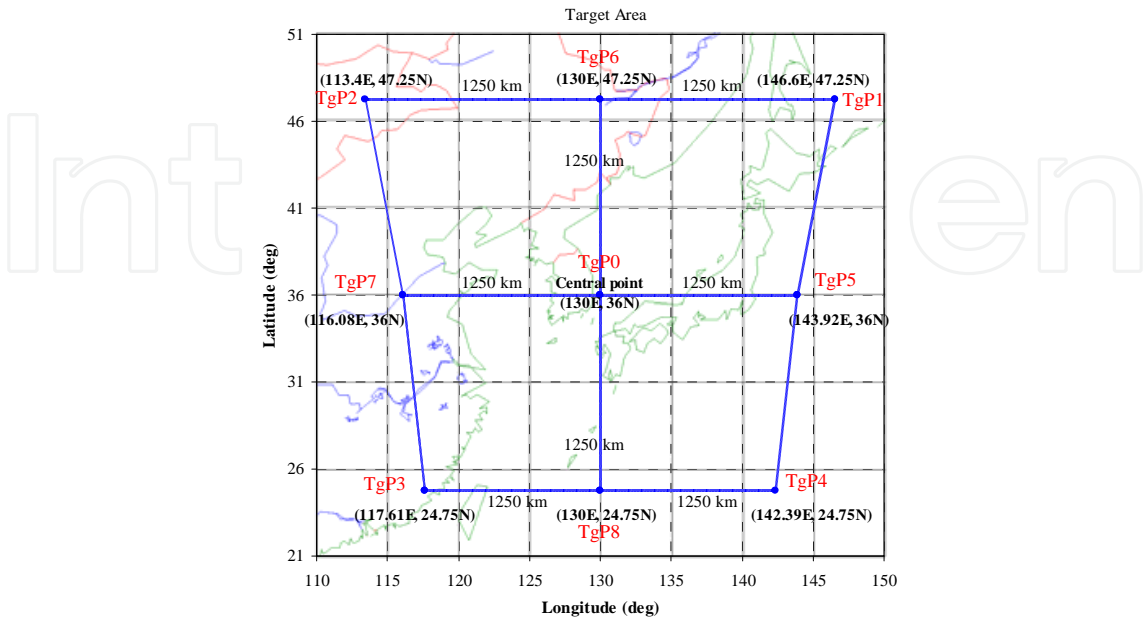


Fig. 6. Target observation coverage of the GOCI

36°N). Such resolution is equivalent to a Ground Sampling Distance (GSD) of 360 m in NADIR direction, on the equator. The GSD is varied over the target area because of the imaging geometry including the projection on Earth and the orbital position of the satellite. The GOCI spectral bands have been selected for their adequacy to the ocean color observation, as shown in Table 2.

| Band | Center | Band-width | Main Purpose and Expected Usage |
|------|--------|------------|--|
| 1 | 412 nm | 20 nm | Yellow substance and turbidity extraction |
| 2 | 443 nm | 20 nm | Chlorophyll absorption maximum |
| 3 | 490 nm | 20 nm | Chlorophyll and other pigments |
| 4 | 555 nm | 20 nm | Turbidity, suspended sediment |
| 5 | 660 nm | 20 nm | Fluorescence signal, chlorophyll, suspended sediment |
| 6 | 680 nm | 10 nm | Atmospheric correction and fluorescence signal |
| 7 | 745 nm | 20 nm | Atmospheric correction and baseline of fluorescence signal |
| 8 | 865 nm | 40 nm | Aerosol optical thickness, vegetation, water vapour reference over the ocean |

Table 2. GOCI spectral bands

2.2.3.2 GOCI design overview

The GOCI consists of a Main Unit and an Electronic Unit. Total GOCI Mass is below 78 Kg. Power needed is about 40W for the electronics plus about 60W for Main Unit thermal control. A Payload Interface Plate (PIP) is part of the Main Unit. It supports a highly stable full SiC telescope, mechanisms and proximity electronics. Fig. 7 shows the main unit which is integrated on the Earth panel of satellite through the PIP. The PIP is larger than the instrument to carry the satellite Infra-Red Earth Sensor (IRES).

The main unit includes an optical module, a two-dimensional Focal Plane Array (FPA) and a Front End Electronics (FEE). The optical module of GOCI consists of a pointing mirror, a Three Mirror Anastigmat (TMA) mirrors, a folding mirror, and a filter wheel. The FEE is attached near the FPA in order to amplify the detector signal with low noise before digitization.

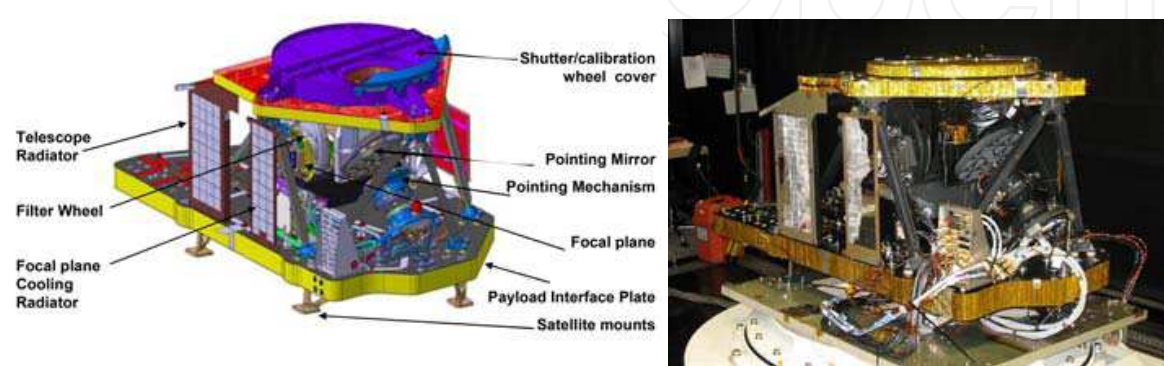


Fig. 7. Design configuration of GOCI main unit and its flight model configuration during integration phase (without MLI)

The shutter wheel is located in front of pointing mirror carrying four elements: shutter which will protect optical cavity during non-imaging period, open part for the ocean observation, Solar Diffuser (SD) and Diffuser Aging Monitoring Device (DAMD) for solar calibration. A Quasi Volumic Diffuser (QVD) has been chosen for the SD and the DAMD among several candidates because it is known to be insensitive to radiation environment. The on-board calibration devices prepared for integration are shown in Fig. 8. The SD covering the full aperture of GOCI is used to perform in-orbit solar calibration on a daily basis. Degradation of the SD over mission life is detected by the DAMD covering the partial aperture of GOCI.



Fig. 8. On-board calibration devices SD, DAMD and pointing mirror mechanism POM

The pointing mirror is equipped with a 2-axis circular mechanism for scanning over observation area. Fig. 8 shows the GOCI pointing mechanism (POM). The pointing mirror is controlled to achieve a Line of Sight (LOS) corresponding to a center of a predefined slot on the Earth. The principle of the pointing mechanism is an assembly of two rotating actuators mounted together with a cant angle of about 1° , the top actuator carrying also the Pointing Mirror (PM) with the same cant angle. When rotating the lower actuator the LOS is moved on a circle and by rotating the second actuator, a second circle is drawn from the first one. It is thus possible to reach any LOS position inside the target area by choosing appropriate angle position on each circle. The mechanism pointing law provides the relation between rotation of both actuators and the LOS with a very high stability. This high accuracy pointing assembly used to select slots centers is able to position the instrument LOS anywhere within a 4° cone, with a pointing accuracy better than 0.03° ($500 \mu\text{rad}$). Position knowledge is better than $10 \mu\text{rad}$ (order of pixel size) thanks to the use of optical encoders. An incident light on the GOCI aperture is reflected by the pointing mirror and collected through the TMA telescope. Then the collected light goes to an optical filter through a folding mirror.

The eight spectral channels are obtained by means of a filter wheel which includes dark plate in order to measure system offset. Fig. 9 shows the filter wheel integrated with eight spectral filters without a protective cover. The FPA for GOCI, which is shown in Fig. 9, is a custom designed CMOS image sensor featuring rectangular pixel size to compensate for the Earth projection over Korea, and electron-optical characteristics matched to the specified instrument operations. The CMOS FPA having 1432×1415 pixels is passively cooled and regulated around 10°C . It is split into two modules which are electrically independent. The GOCI electronics unit, which is shown in Fig. 9, is deported on satellite wall about 1.5m from the GOCI main unit. It provides control of mechanisms (pointing mirror, shutter wheel, filter wheel), video data acquisition, digitization, mass memory and power.

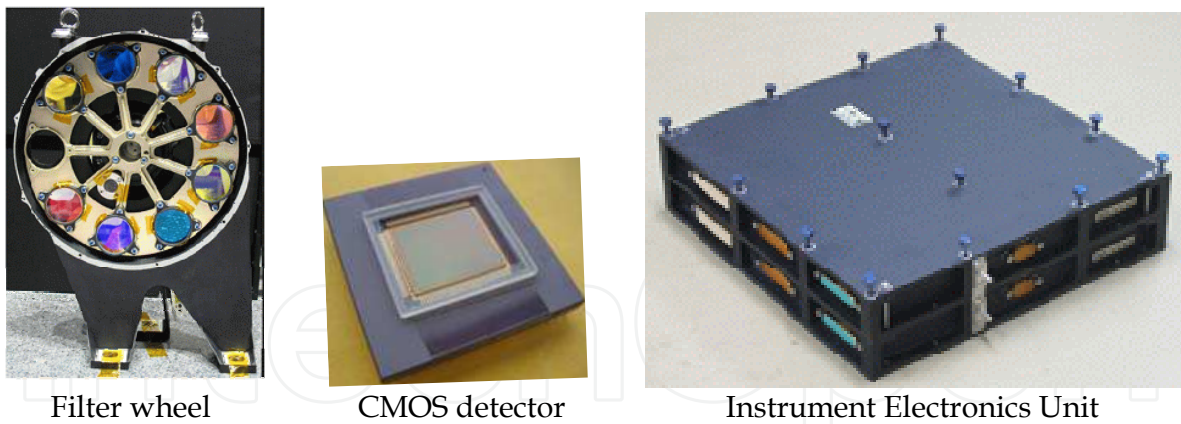


Fig. 9. GOCI filter wheel without cover, CMOS detector package with temporary window and Electronics Unit

The imaging in GOCI is done in the step and stare fashion, passing along the 16 slots, as shown in the Fig. 10.

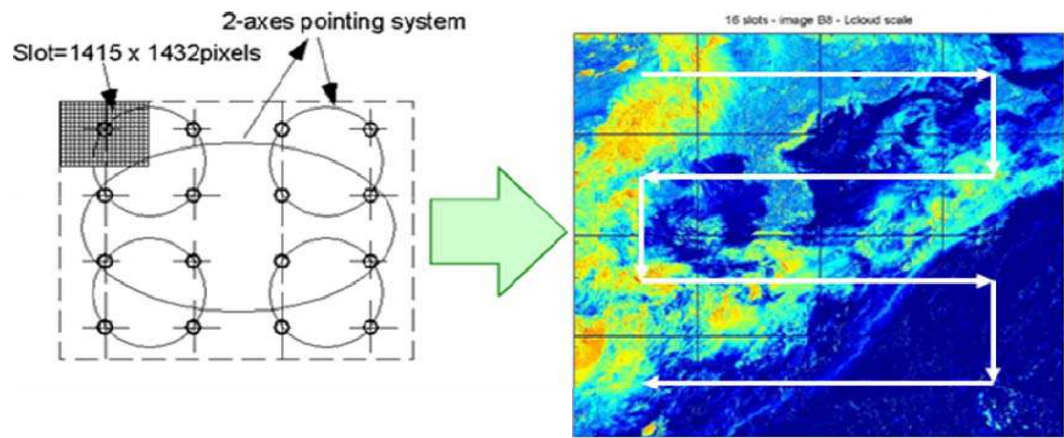


Fig. 10. GOCI imaging principle

2.2.4 COMS INR system

2.2.4.1 Overview of COMS INR system

Achieving and maintaining a good geo-localization of the images on the ground is an essential part of the geostationary remote sensing satellite for the utilization of the remote sensing data to be a meaningful and fruitful one. To this purpose, the Image Navigation and Registration (INR) system should be in place, and in COMS, a novel approach to INR was developed, allowing a-posteriori location of the images on the geoid based on automatic identification of landmarks and comparison with a reference database of specific terrestrial features such as small islands, capes, and lakes.

In this novel approach, INR is not directly dependent on the satellite and payload models and hence can avoid any indispensable modeling and prediction error in the process. The high reliance on the landmarks and the acquisition of sufficient number of good-quality landmarks, however, become the key part of the design in this approach and such acquisition must be secured for this approach to be practically successful. In COMS INR,

excellent landmark matching algorithm, fine-tuning of configuration parameters during IOT and the fine-tuning of newly established landmark database with ample landmark sites at the final phase of IOT rendered such acquisition of sufficient number of good landmarks.

Fig. 11 shows the overall architecture of COMS INR. All the processing are done on ground except for the long term image motion compensation (LTIMC) and as can be seen here, the whole INR system is operated in close conjunction with the AOCS.

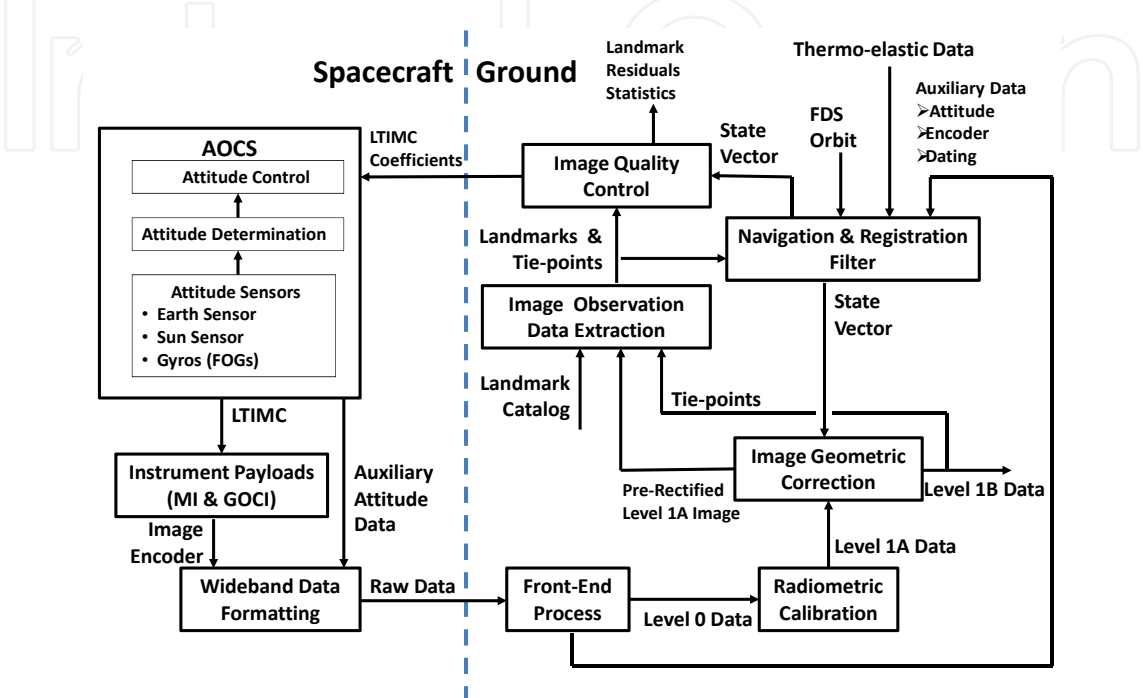


Fig. 11. COMS INR overall architecture

2.2.4.2 Description of COMS INR system and processing

In this section, the description of each module and each processing which comprises the whole COMS INR system, as shown in the Fig. 10, is provided.

2.2.4.2.1 Space Segment INR

Attitude determination

The on-board attitude determination estimates the spacecraft attitude from attitude sensors measurements (IRESs, Sun Sensors and FOGs) through filtering process. This process is performed at 10 Hz and sub-sampled at 1 Hz to insert into the MI wideband telemetry for use by the Navigation and Registration Filter Module on ground.

Attitude control

The on-board attitude control loop actuates momentum wheels, solar array, and thrusters. The control loop is designed to be robust to effect of disturbances on MI & GOCI field of views. Disturbances include:

- Diurnal attitude pointing perturbation due to thermo-elastic distortion and solar torques.
- Thruster firing for station keeping and wheel off-loading.

Long term image motion compensation (LTIMC)

The on-board LTIMC is used to compensate pointing bias and long term evolutions (seasonal, ageing) to keep the area to be observed within the MI & GOCI field of views.

Wideband data formatting

Wideband data consists of MI & GOCI imagery/telemetry and AOCS auxiliary attitude data.

2.2.4.2.2 Ground Segment INR

The image observation data extraction module

This module gathers all functions of data extraction from images: cloud cover detection, landmark detection from image/database matching, multi-temporal tie point detection from image/image matching, and multi-spectral tie point detection from band-to-band matching. A first “pre - rectification” of Level 1A images allows retrieving 2D local image coherence.

The navigation and registration filter module

This module gathers all functions of geometric models: localization model (including focal plane and scan mirror models), navigation filter, landmarks or tie points position prediction. This module performs state vector estimation through a hybridization filter that combines landmarks, thermo-elastic, orbit, and gyros data in the way that minimizes criteria on landmarks (for navigation) or tie points (for registration) residuals.

The image geometric correction module

This module gathers all functions relative to image resampling and Modulation Transfer Function (MTF) compensation. For each pixel of an image, the state vector allows computing the shift between raw geometry and reference geometry. Each pixel of the Level 1B image is computed through radiometric interpolation with respect to the neighbouring pixels around its corresponding pixel in the Level 1A image.

The image quality control module

Once the state filter estimation is performed, ground pixels corresponding to landmarks are localized. The result difference with respect to the landmark known position is called “residual”. It can be done on the landmark used for navigation, but also on “reference landmarks” which are used for the navigation accuracy control filter. All computed residuals are stored for further statistics. The statistics (average, standard deviation, max value) on residuals within the image gives instantaneous INR performance. The statistics over a set of image during a certain period gives INR performance relative to the period. The statistics relative to a specific landmark over a certain period gives information on quality and reliability for that landmark. This result will be used to periodically update landmark database with confidence rate that has to be taken into account for better accuracy of the navigation filter. All statistics are also computed with respects to context: date, time, cloud conditions.

2.2.5 COMS ground segment

The COMS GS (Ground Segment) consists of four GCs (Ground Centers); Satellite Control Center (SOC), National Meteorological Satellite Center (NMSC), Korea Ocean Satellite Center (KOSC), and Communication Test Earth Station (CTES) (KARI, 2006).

The SOC performs the primary satellite operation/monitoring and the secondary image data processing. The NMSC and KOSC have a role of the primary image data processing for MI (in NMSC) and GOCI (in KOSC), respectively, and The NMSC is also the secondary ground center for a satellite operation/monitoring. The CTES monitors RF (Radio Frequency) signals to check the status of Ka-Band communication system.

The SOC has two functions of the COMS GS; MI/GOCI Image data processing (as the backup center) and satellite operation/monitoring (as the primary center). One of SOC function is implemented in IDACS (Image Data Acquisition and Control System) for Image data processing by three subsystem; DATS (Data Acquisition and Transmission Subsystem), IMPS (IMage Pre-processing Subsystem), and LHGS (LRIT/HRIT Generation Subsystem) (Lim et al., 2011).

The other SOC function, satellite operation and monitoring, is implemented in SGCS (Satellite Ground Control System) by five subsystems; MPS (Mission Planning Subsystem), TTC (Telemetry, Tracking, and Command), ROS (Real-time Operations Subsystem), FDS (Flight Dynamics Subsystem), and CSS (COMS Simulator Subsystem) (Lee et al., 2006).

Fig. 12 shows the essential architecture of COMS ground segment with key composing subsystems and Table 3 describes functions of subsystem for COMS ground segment; DATS, IMPS, LHGS (IDACS) MPS, TTC, ROS, FDS, and CSS (SGCS).

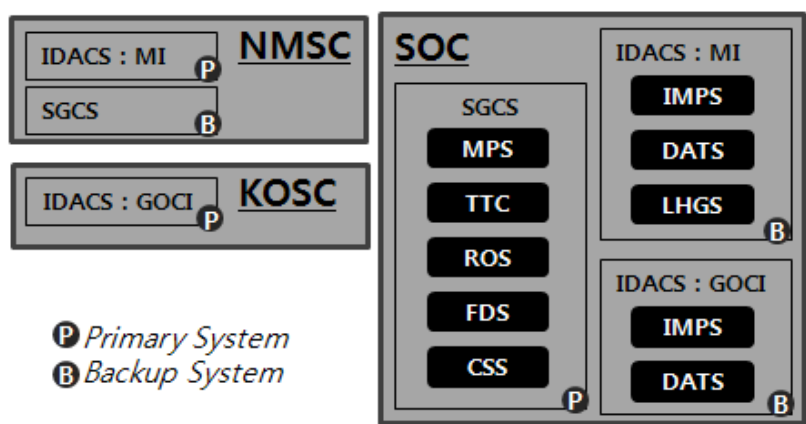


Fig. 12. COMS ground segment architecture with key composing subsystems

| System | Sub-System | Functions |
|--------|------------|--|
| IDACS | DATS | Reception and error correction of CADU Processing and dissemination of LRIT/HRIT Control and monitoring of IDACS |
| | IMPS | CADU receiving and processing Radiometric correction (IRCM) Geometric calibration (INRSM) Payload status monitoring Interfaces among subsystems of the IDACS |
| | LHGS | LRIT/HRIT generation Compression and encryption for LRIT/HRIT generation |

| System | Sub-System | Functions |
|--------|------------|---|
| SGCS | MPS | Mission request gathering Mission scheduling Mission schedule reporting |
| | TTC | Telemetry reception Command transmission Tracking and ranging Control and monitoring |
| | ROS | Telemetry processing Telemetry analysis Command planning Telecommand processing |
| | FDS | Orbit Determination and prediction Station-keeping and re-location planning Satellite event prediction Satellite fuel accounting |
| | CSS | Satellite dynamic static simulation Command verification Anomaly simulation |

Table 3. Functions of the COMS ground segment

3. COMS in-orbit performances

3.1 COMS AOCS performances and platform stability

The quality of images taken by on-board optical instruments is strongly dependent on the quality of the platform stabilisation. Three (3) strong requirements have been put on the COMS platform, all necessary to obtain the specified image quality.

- pointing accuracy (pitch and roll) : this specification is essential to a priori know where the instrument line of sight is aiming at. This is important for Ka band payload operations, for GOCI operation (due to further stitching of small images to construct the large imaging area) and for MI which can be commended to frequently review some local areas.
- pointing knowledge (pitch and roll) : the pointing knowledge is mainly driven by the INR in order to start the landmark matching processing with a sufficient accuracy.
- pointing stability (pitch and roll) : this specification is mainly driven by the GOCI instrument, requesting integration times as long as 8 seconds, with a jitter less than 10μrad.

The first point is fulfilled by the heritage bus (E3000 platform), but the two last points have necessitated the implementation of a high precision Fibre Optic Gyro (Astrium’s FOG Astrix 120 HR), furthermore the third point has been flown down to micro-vibration dampers under wheels, various AOCS tuning (solar array natural mode damping, optimised wheel zero crossing management), optimized manoeuvres (reaction wheel off loading, EW and NS manoeuvres, etc.), and few operational constraints (stop solar array rotation during GOCI imaging period, etc.).

The resulting performances are typified as the pointing knowledge of better than 0.003° , the pointing accuracy of better than 0.05° , and the pointing stability of better than $7\mu\text{rad}/8\text{s}$, all in roll and pitch. Fig. 13 shows the typical example of the performance on the platform stability.

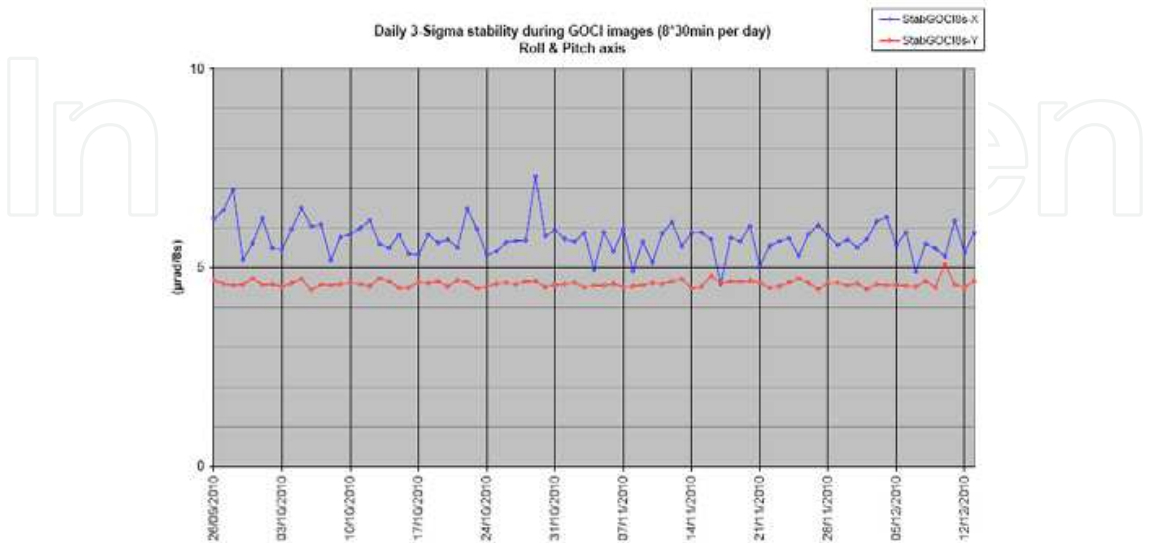


Fig. 13. COMS platform stability, as measured for a period of 3 months and computed on a 3-sigma basis

3.2 Radiometric performances of MI and GOCI

3.2.1 MI radiometric performances

3.2.1.1 MI in-orbit SNR

From the MI Visible dark noise analysis results, COMS MI in-orbit SNR at 5% albedo have been computed for both side 1 and side 2 of MI and the in-orbit SNR in both sides proved to be better than on ground measurement and significantly above the specification, $\text{SNR} > 10$ at 5% albedo. Table 4 shows both the on-ground and in-orbit SNR at 5% albedo for MI side 1.

| MI Side 1 | SNR 5% | |
|------------|-----------|----------|
| | On Ground | In Orbit |
| Detector 1 | 24 | 27.18 |
| Detector 2 | 24 | 26.28 |
| Detector 3 | 23 | 26.20 |
| Detector 4 | 24 | 27.01 |
| Detector 5 | 23 | 25.24 |
| Detector 6 | 23 | 27.08 |
| Detector 7 | 23 | 26.00 |
| Detector 8 | 24 | 26.21 |

Table 4. MI On-Ground and In-Orbit SNR results, MI side 1

3.2.1.2 MI in-orbit radiometric calibration

COMS IOT (In-Orbit Test) MI calibration activities were divided into two main parts: MI visible channel and infrared channel calibrations. The visible channel calibration was conducted from July 11, 2010 after the COMS Launch (2010.6.26. 21:41 UTC). Calibration activity of the Infrared channels including the visible one was started from Aug 11, 2010 after the completion of the out-gassing (removal of remnant volatile contaminants by heating). The functional and performance tests were performed for both two functional sides (SIDE1: primary, SIDE2: secondary) plus two patch temperatures (patch Low and Mid) of the MI payload. In addition to the images of MI channels, albedo monitor and moon images were also acquired and analyzed. The final performance verification was checked officially at the phase 1 & phase 5 end meeting (Jan 26, 2011) after the intensive MI radiometric calibration processes conducted from July, 2010 to Jan, 2011. Summary of the verifications at the meeting is listed as follows.

- 1. Command and control tests for both sides (Side 1/Side2) were successful
- 2. Scan mechanism tests were successful
- 3. Image monitoring and acquisition tests were successful
- 4. The performance tests of MI visible channel were successful
- 5. The performance tests of MI infrared channels based on the payload real-time operational configuration modes were successful

3.2.1.2.1 MI visible channel calibration process

As shown in Fig. 14, the MI visible channel calibration process was simply verification of a linear visible calibration equation using the real data sets. After that, necessity of the normalization among eight detectors was checked. Albedo monitor data analysis and moon image processing were used for the detector's trend monitoring.

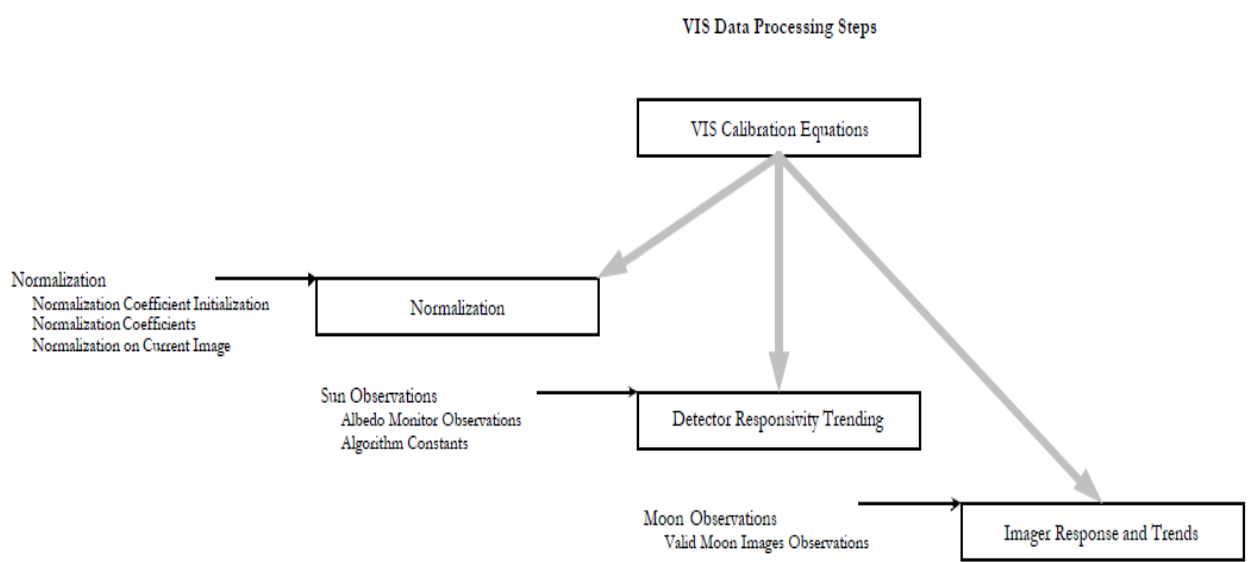


Fig. 14. MI visible channel radiometric calibration process flow chart

The pixel-to-pixel response non-uniformity (PRNU) were examined using the both space look and image data (Fig. 15). PRNU met the requirement specifications (denoted by red

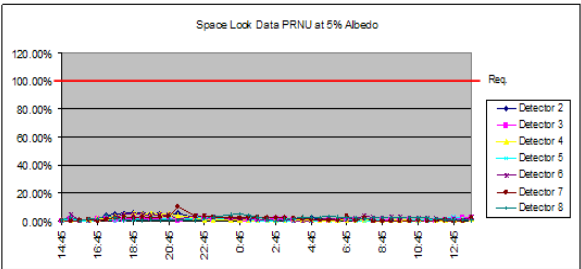


Fig. 15. PRNU Check (SIDE1): Space-Look data

lines). As a result, the normalization algorithm was not implemented on the visible channel calibration process.

3.2.1.2.2 MI infrared channel radiometric calibration

Different from the visible channel, the MI infrared channel calibration process has complex steps to get qualified data as shown in Fig. 16. First, coefficients of the basic (nominal) IR calibration equation were verified using the real data sets and then four major steps were taken: 1) Scan mirror emissivity compensation, 2) Midnight effect correction, 3) Slope averaging and 4) 1/f noise compensation.

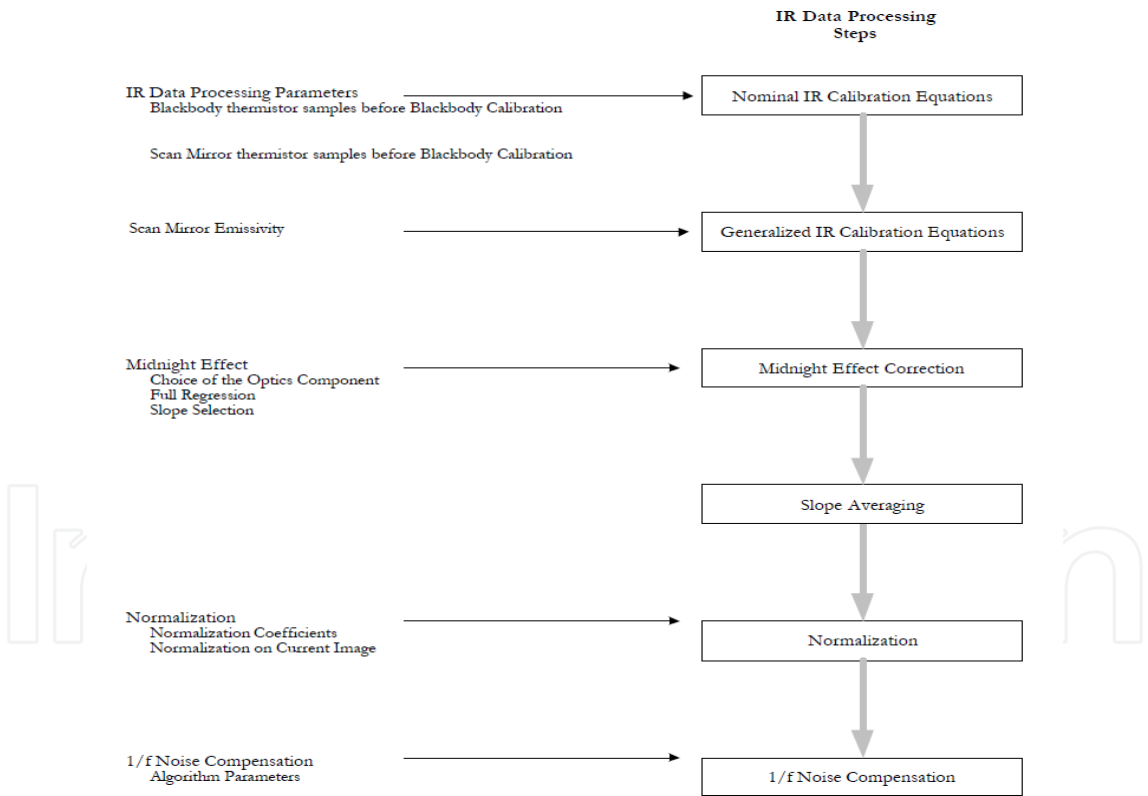


Fig. 16. MI infrared channel radiometric calibration process flow chart

1. Scan mirror emissivity correction

Based on the scan mirror emissivity (as a function of a scan angle), the effect of emitted radiances from the coating material on the scan mirror were compensated. The computed scan mirror emissivities according to different scan angles are shown in Fig. 17.

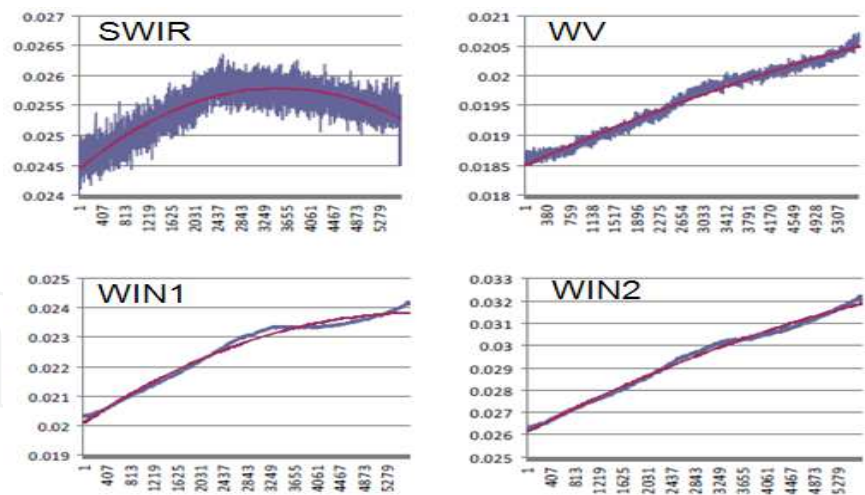


Fig. 17. Computation of the scan mirror emissivity for four different infrared channels (1Dark Image, Side1, Patch Low, Det A, 2010.8.16).

2. Midnight effect compensation

Before and after four hours of near local midnight data were corrected using a mid night compensation algorithm (see Fig. 18). The estimated slope(open circles and squares) based on the regression between the black body slope and the selected optic temperature were used near midnight and the original slope values(thick lines) are used during the rest of time.

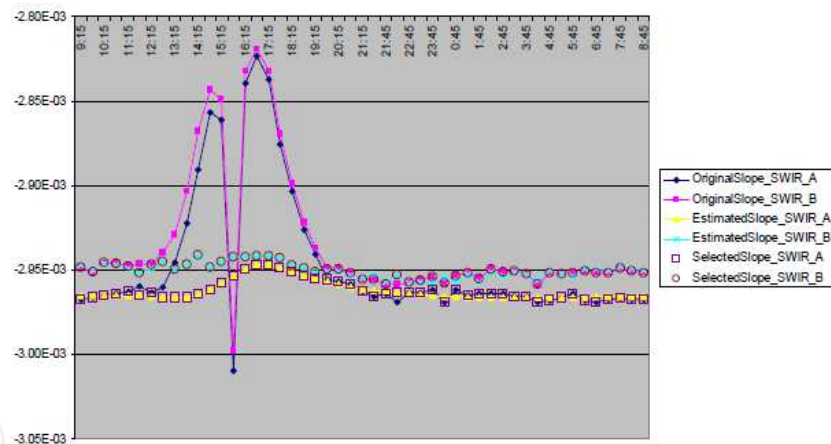


Fig. 18. IR Midnight Effect: the result of slope selection (SWIR; Side 1/Patch Low)

3. Slope averaging

Slope averaging is a smoothing process to remove the responsivity variation of the detectors due to the diurnal variation of background radiation inside the sensor. The reference slope value were compared to that of the previous day and the residual between two were filtered by the slope averaging.

4. 1/f noise compensation

The 1/f noise compensation, which is a filtering of random noise on the lower frequency components was also conducted. After the 1/f noise compensation, the stripping effects on the water vapor channel were greatly removed.

3.2.1.2.3 The result of the MI IOT radiometric calibration processes

The PRNU values from the radiometric indices computed from the real time MI data processing system of COMS (called IMPS) indicated that relative bias between detectors of infrared channels were minimal and thus the normalization process step on the infrared channels were skipped as same as the visible one. The complete COMS MI images resulted from the IOT (see Fig. 19) showed that the radiometric performance of the MI payload meets the all requirement specifications for the current operation configuration of MI (SIDE 1, Patch Low).

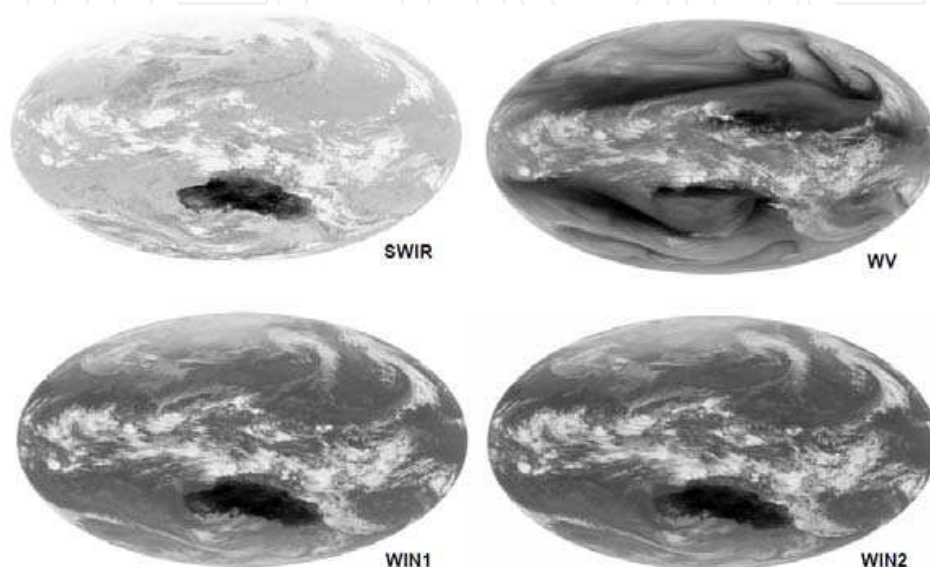


Fig. 19. Calibrated MI FD Level 1A images (before INR), (Side 1, Patch Low, 2010.12.23)

3.2.2 GOCI radiometric performances

3.2.2.1 GOCI in-orbit SNR

The GOCI was turned on for the first time in orbit on July 12, 2010 and captured its first image the day after. Both sides (primary and redundant) were successfully tested during about two weeks. After the successful functional tests such as the mechanism movement, detector temperature control, and imaging chain validity, the radiometric performance tests and radiometric calibration tests have been performed. The radiometric performance test is aimed to verify the validity of performance measured on ground. In-orbit offset and dark signal shows a quite good correlation with the ground measurements. Also the radiometric gain matrix, which has been measured in-orbit, is very similar to the ground gain. The SNR test results, which are provided in Table 5, show the performance exceeding the requirements in all 8 spectral bands by 25 to 40%. This is mainly due to the excellent quality of the CMOS matrix detector, and the design margin considered for worst case analysis.

3.2.2.2 GOCI in-orbit radiometric calibration

GOCI in-orbit radiometric calibration relies on a full pupil Sun Diffuser (SD), made of fused silica, known to be insensitive to radiations. The instrument is designed to allow a calibration every day. In practice, during IOT, two calibrations per week were performed. After IOT, the frequency of calibration was reduced to one per week. The

| Band | Mean SNR | SNR specification at GOCI level |
|------|----------|---------------------------------|
| B1 | 1476 | 1077 |
| B2 | 1496 | 1199 |
| B3 | 1716 | 1316 |
| B4 | 1722 | 1223 |
| B5 | 1586 | 1192 |
| B6 | 1513 | 1093 |
| B7 | 1449 | 1107 |
| B8 | 1390 | 1009 |

Table 5. GOCI In-Orbit SNR test result

potential aging of the SD is monitored by a second diffuser (Diffuser Aging Monitoring Device: DAMD) used less frequency than the SD, typically once per month since the end of the IOT. When not in used, both SD and DAMD are well protected by the shutter wheel cover to minimise their exposure to the space environment.

Through IOT period, about six months, the instrument calibration and the calibration stability were fully verified. The purpose of radiometric calibration test is to verify the in-orbit calibration method which is based on two point measurements (Kang & Coste, 2010). The in-orbit radiometric gain matrix of GOCI is calculated by using two sun images, which are obtained through the SD with two different integration times. The imaging time for the sun has been specified according to the desired solar incident angle over 25 degree to 35 degree. The actual solar incident angle of measured sun image is calculated by using the On-Board Time (OBT) which is included in the secondary header of the raw data. During IOT, sun imaging for eight spectral bands has been performed over two days based on one week period. For each calibration, six sets of sun images with short and long integration time have been obtained for each spectral band over about 10 minutes. Variation of gains calculated by 6 sets are very small (0.1 % to 0.3%) and are most probably due to processing noise (small errors in the ephemerides and in the calibration time) and also possibly to short term variations of the sun irradiance. Fig. 8 shows the gain evolution over eight months. For first three months, the gain shows a relatively rapid decrement. There is about 2% variation over eight months. Fig. 20 shows the aging factor of the SD over eight months. The trend provided in this Figure shows a sinusoidal variation over 8 months with about maximum

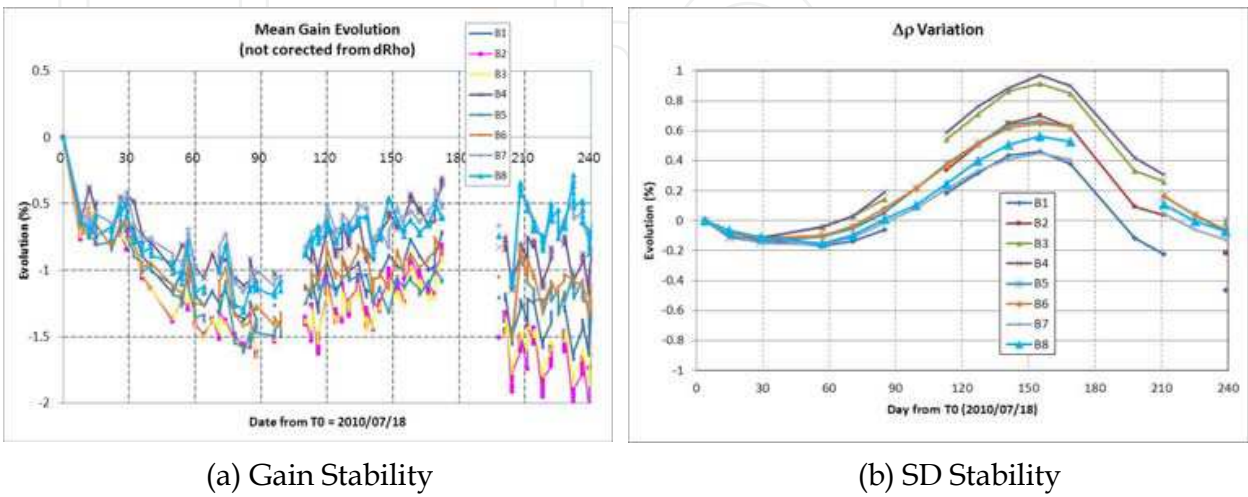


Fig. 20. In-orbit radiometric stability over 8 months

1% amplitude. This is probably not the real variation of SD. In addition the longitudinal solar incident angle to the GOCI shows the similar variation over the year. The reason for this sinusoidal variation is now under examination. The variations lower than 1% over almost one year shows the SD stability. All the variations observed in orbit up to now are within 1 to 2% which is very low and very satisfactory. Some evolutions seem to be correlated with the longitudinal solar incident angle. This opens the way to further improvement of the calibration model if necessary.

The major performances (Modulation Transfer Function - MTF and Signal to Noise Ratio - SNR) are presented in this chapter, all other performances being well within the requirements.

One of the major advantages of ocean observation with the GOCI is that continuous monitoring is possible with images provided every hour, which maximizes chance of clear observation of the whole field even in cloudy season. No sun glint occurs thanks to the angular position of the field of view during daytime, while it discards many observations in low orbit.

3.3 Spatial and geometric performances of MI and GOCI

3.3.1 GSD and MTF

3.3.1.1 MI

During IOT, the MI Ground Sampling Distance (GSD) and the spatial performance (MTF) have been fully checked and verified. The GSD has been verified as follows. The landmark matching results by the INRSM were used and the angular steps in both E/W and N/S were measured by best fit between level 1A image coordinates and landmark GEOS positions. Those angular steps were used to determine a projection function for each image (or sub-image). Then, the specified GSD at Nadir was verified using the relevant projection function.

Table 6 shows the measured MI MTF results.

| MTF | Side 1 | | Side 2 | | Required Minimum |
|---|--------|------|--------|------|------------------|
| | EW | NS | EW | NS | |
| 0.25 Nyquist normalized wrt IFOV, i.e. 28μrad | 0.93 | 0.98 | 0.92 | 0.98 | 0.87 |
| 0.50 Nyquist normalized wrt IFOV, i.e. 28μrad | 0.83 | 0.92 | 0.83 | 0.92 | 0.68 |
| 0.75 Nyquist normalized wrt IFOV, i.e. 28μrad | 0.68 | 0.74 | 0.69 | 0.72 | 0.49 |
| 1.00 Nyquist normalized wrt IFOV, i.e. 28μrad | 0.52 | 0.45 | 0.54 | 0.47 | 0.20 |

Table 6. Measured In-Orbit MI MTF

3.3.1.2 GOCI

During IOT, the GOCI GSD has been verified by the same method as with MI, and the imaging coverage and the slot overlap have also been fully verified. The spatial performance (MTF) has also been checked. Before launch, the GOCI MTF performance was tested through ground test at the payload level. The in-orbit MTF test would allow the validation of MTF at system level including the satellite stability performance. But the measurement accuracy for in-orbit test is much worse than the ground test depending on the availability and the quality of the transition patterns between bright and dark in the image. The GOCI

MTF is calculated by using the image having a radiometric transition (such as a coast line) which is equivalent to Knife Edge Function (KEF) measurement. Table 7 shows the GOCI MTF test result. Significant margins are demonstrated with respect to specifications; similar margins are present in all spectral bands.

| MTF @ Nyquist | Band 8 | | | |
|------------------------|--------|------|------|------|
| | E | W | N | S |
| Sample #1 | 0.34 | 0.42 | 0.38 | 0.30 |
| Sample #2 | 0.27 | 0.43 | 0.37 | 0.36 |
| Sample #3 | 0.29 | 0.33 | 0.42 | 0.33 |
| Sample #4 | 0.28 | 0.45 | 0.37 | 0.32 |
| Sample #5 | 0.35 | 0.37 | 0.37 | 0.26 |
| Sample #6 | 0.40 | 0.42 | 0.38 | 0.31 |
| Sample #7 | 0.31 | 0.44 | | |
| Sample #8 | 0.43 | 0.34 | | |
| Sample #9 | 0.32 | 0.28 | | |
| Sample #10 | 0.32 | 0.36 | | |
| Mean Value | 0.36 | | 0.35 | |
| Standard Error | 0.06 | | 0.04 | |
| Specification | 0.30 | | 0.30 | |
| (Mean - Spec.) / Spec. | 19% | | 16% | |

Table 7. Measured GOCI MTF in the band 8

3.3.2 INR performances

The INR IOT took a significant amount of time, as the final tuning requested. The first positive result obtained from the first images was the number of landmarks automatically extracted by the INR software. During the development, it had been demonstrated that a minimum of typically 100 landmarks were necessary, and sometimes more than 600 landmarks could be found on images.

The INR performance is evaluated on the basis on land marks residuals (statistical error after landmark best fit). In order to verify the validity of this approach, the coast line from the images is checked against an absolute coast line (based on GSHHS). The following figures in the Table 8 illustrate the typical performances of COMS INR as observed during the IOT.

| | Navigation | | Within Frame Reg. | | Registration 15-min | | Registration 90-min | |
|----------------------------|------------|------|-------------------|-------|---------------------|------|---------------------|-------|
| | EW | NS | EW | NS | EW | NS | EW | NS |
| Specification | 56.0 | 56.0 | 42.0 | 42.0 | 28.0 | 28.0 | 42.0 | 42.0 |
| Spec + Allocation VIS only | 65.3 | 65.3 | 63.4 | 63.4 | 55.2 | 55.2 | 63.4 | 63.4 |
| Jan 2011, VIS only | 43.0 | 35.6 | 52.1 | 46.2 | 26.8 | 23.4 | 27.4 | 24.5 |
| Sep 2010, VIS only | 31.8 | 30.5 | 39.5 | 42.7 | 16.0 | 17.5 | 19.2 | 19.5 |
| Spec + Allocation VIS & IR | 87.5 | 87.5 | 103.9 | 103.9 | 99.1 | 99.1 | 103.9 | 103.9 |
| Jan 2011, VIS & IR | 46.3 | 43.7 | 58.8 | 55.8 | 39.8 | 37.7 | 33.4 | 33.2 |
| Sep 2010, VIS & IR | 40.5 | 40.6 | 50.6 | 54.1 | 23.9 | 23.8 | 27.1 | 27.4 |

| | Navigation | | Within Frame Reg. | | Frame-to-Frame | | Band-to-Band | |
|----------------------------|------------|------|-------------------|------|----------------|------|--------------|------|
| | EW | NS | EW | NS | EW | NS | EW | NS |
| Specification | 28.0 | 28.0 | 28.0 | 28.0 | 28.0 | 28.0 | 7.0 | 7.0 |
| Spec + Allocation VIS only | 31.3 | 31.3 | 34.3 | 34.3 | 34.3 | 34.3 | 21.0 | 21.0 |
| Jan 2011 | 17.5 | 15.5 | 22.9 | 21.2 | 7.7 | 7.3 | <10.0 | <9.6 |

Table 8. COMS MI and GOCI INR performances (units in µrad)

Worth noting is the fact that the COMS AOCS pointing performances, as described in section 3.1, provide a significant contribution to the final INR performances. Also worth noting is the timeliness requirement put on the MI INR processing. As mentioned in section 2.2, the satellite serves as telecommunication relay to broadcast corrected data to end users in international formats called HRIT and LRIT. Both formats suppose to rectify the data both radiometrically and geometrically. An allowance of 15 minutes is given to perform the ground processing before uploading again the data to the satellite. After few inevitable tunings, the whole process is now performed in typically 12 minutes. For illustration purpose, two examples of shoreline matching are presented for MI vis channel and for one GOCI spectral band in the Fig. 21 and Fig. 22.

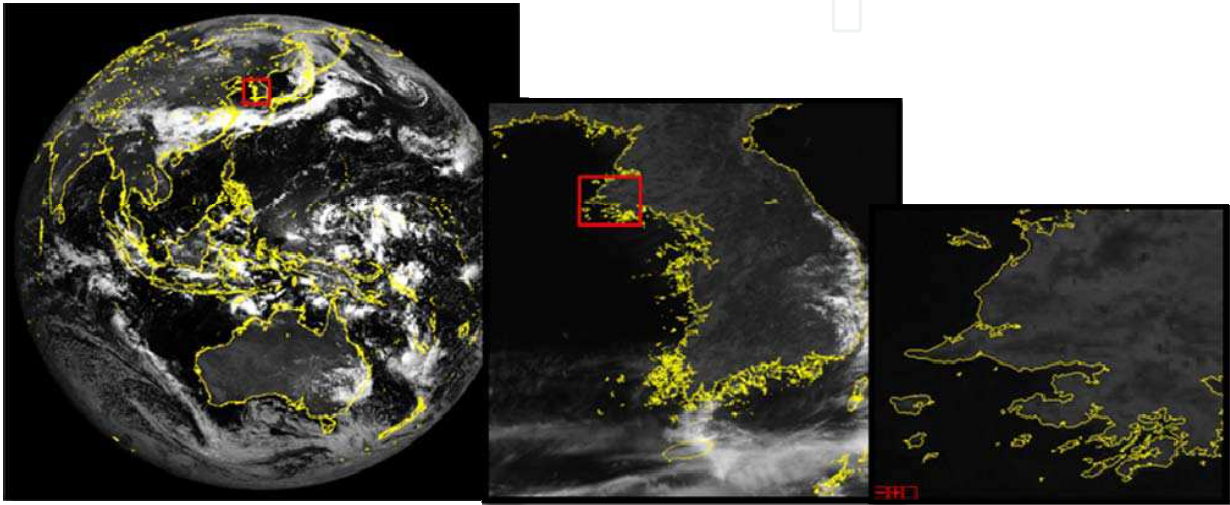


Fig. 21. MI shoreline matching (FD, VIS)

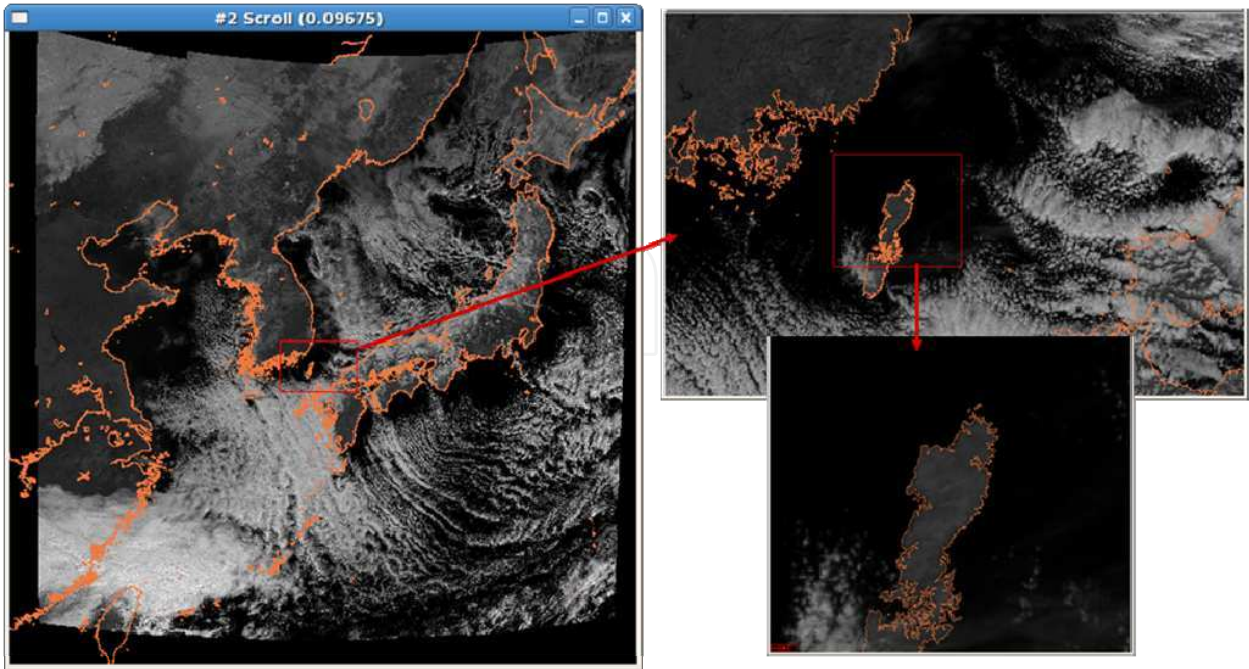
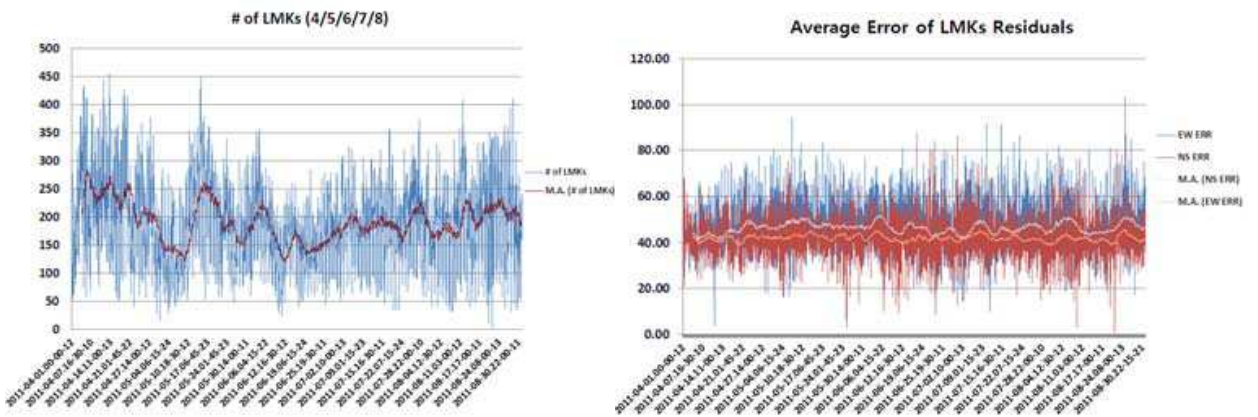


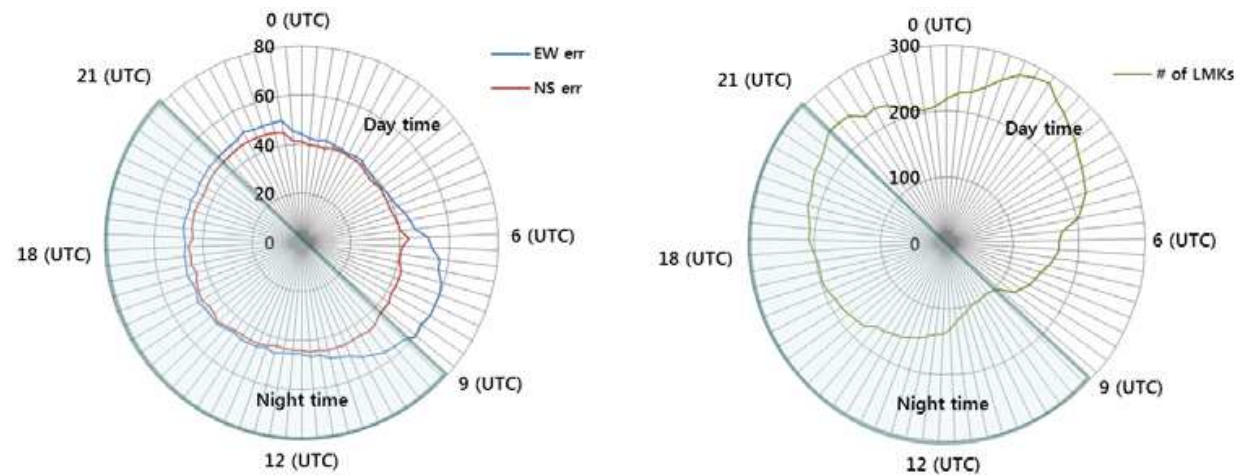
Fig. 22. GOCI shoreline matching. The reference shoreline is superimposed to the geometrically rectified GOCI image. Matching is better than 2 pixels over the whole area.

Further analysis and monitoring on INR performances have been performed since the start of normal operation of COMS for the service to the end users, and Fig. 23 and Fig. 24 illustrate some of these typical COMS INR performances.



Mode: ENH, Channel: VIS and IR, and negative correlation between the number of LMKs and the average of Residuals (courtesy of KMA)

Fig. 23. MI INR performance during 1st April ~ 31th August.



Mode: ENH, Channel: VIS and IR, and negative correlation between the number of LMKs and the average of Residuals: Twilight effects (courtesy of KMA)

Fig. 24. MI INR performance during 1st April ~ 31th August.

4. Application and suggestion

It has been merely 8 months since the outset of the normal operation of COMS for the distribution and service of the images and image products to the end users and scientific communities. The activities in this period in terms of the data processing, calibration and the end product generation and the related studies and researches have been exceedingly interesting, proactive and imaginative, to say the least, and in a word ‘dynamic’ in a very positive and rewarding sense. This section describes the application aspect of the COMS image data from MI and GOCI, addresses some posing technical challenges at the present time on this course of data application, summarizes some of the representative end products both from MI and GOCI and discusses the way forwards with some suggestions.

4.1 MI

4.1.1 Generation of MI end products

As mentioned in the previous sections, COMS MI Level 1B data are generated through radiometric and geometric calibrations and then sixteen meteorological products(level 2) are produced by CMDPS (COMS Meteorological Data Processing System) as shown Fig. 25.

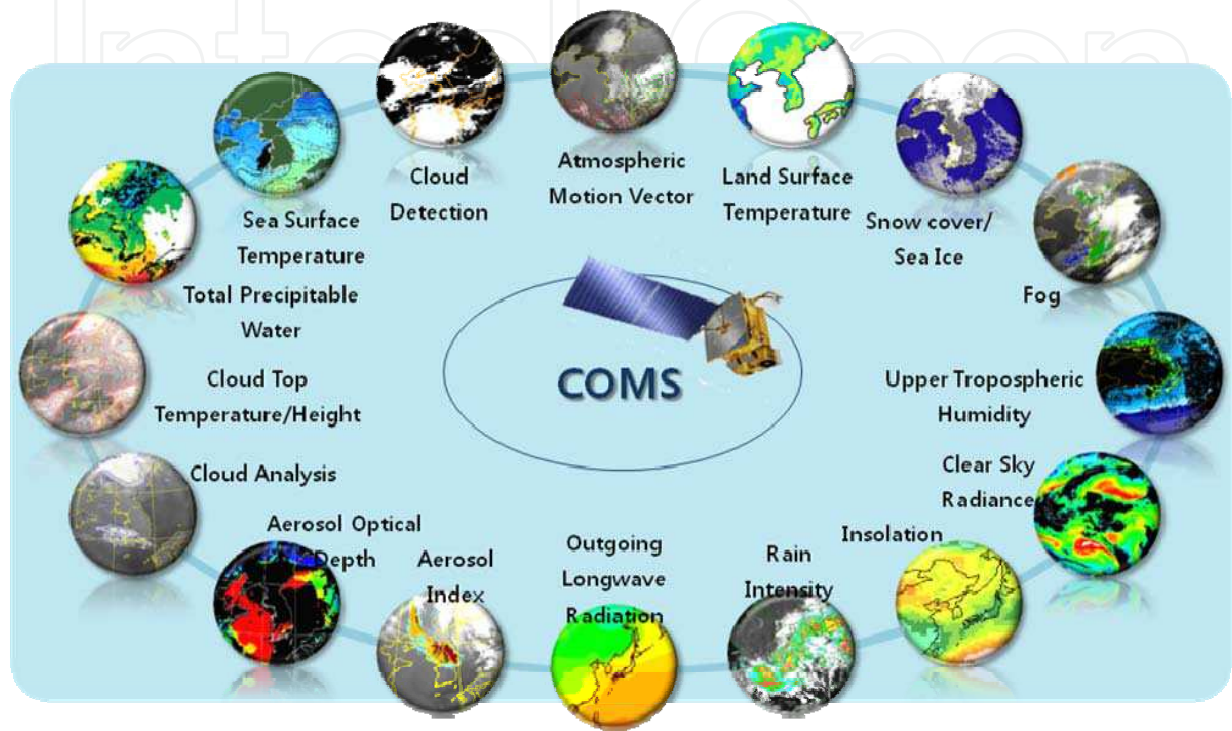


Fig. 25. COMS Meteorological Products

Parts of meteorological products from COMS MI have been generated operationally since April 1, 2011 together with COMS operation. Those products are cloud analysis (type, phase and amount), cloud top temperature/pressure, atmospheric motion vector, cloud detection, fog, and aerosol index. And then, four products, which are sea surface temperature, rain

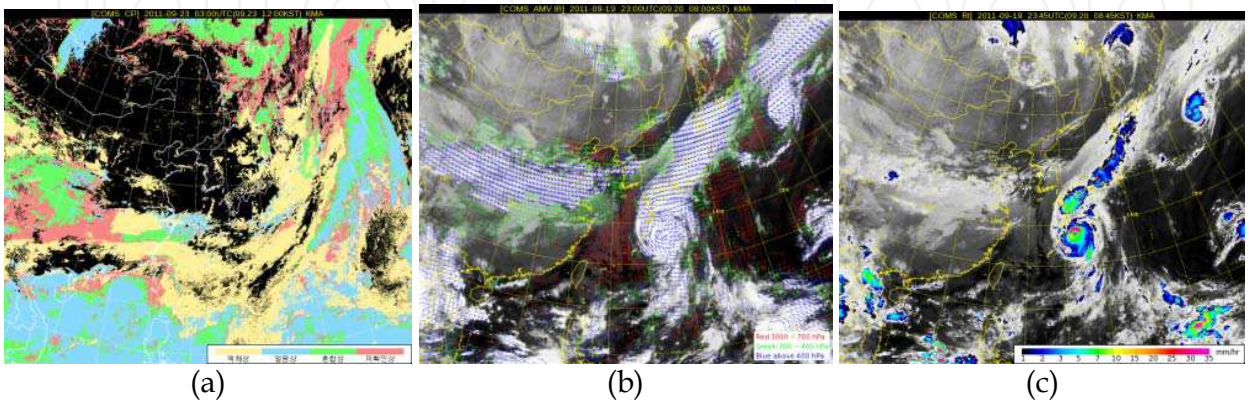


Fig. 26. Examples of COMS meteorological products (a) cloud phase (b) atmospheric meteorological vector and (c) rain intensity.

intensity, outgoing longwave radiation, and upper tropospheric humidity, were generated additionally from 10 August 2011. These products are currently being validated through comparison between satellite-derived products and ground in-situ data. For example, detection area of Asian dust (aerosol index) occurred in 2011 April and May was compared with COMS GOCI and MODIS (Moderate Resolution Imaging Spectroradiometer) true color images or OMI (Ozone Monitoring Instrument) AOD (Aerosol Optical Depth). The other six products which are land surface temperature, sea ice/snow cover, total precipitable water, insolation, clear sky radiance, and aerosol optical depth will be operationally produced soon.

4.1.2 Application to weather forecasting and analysis

In Korean peninsula, annual losses and damages in human and material are enormous due to the convective cloud accompanying summer heavy rainfall, which is either flown from the West Sea or originated locally. COMS can monitor and watch the origination and development of this convective cloud since it can observe Korean peninsula with MI in a concentrative way eight times an hour. NMSC is supporting the weather forecasting with the developed technique for Very Short Range Forecasting utilizing COMS MI meteorological data, which was introduced and derived from the technique of convective cloud rainfall intensity calculation and monitoring by the SAFNWC (Satellite Application Facilities Nowcasting) of EUMETSAT (European Organization for the Exploitation of Meteorological Satellites).

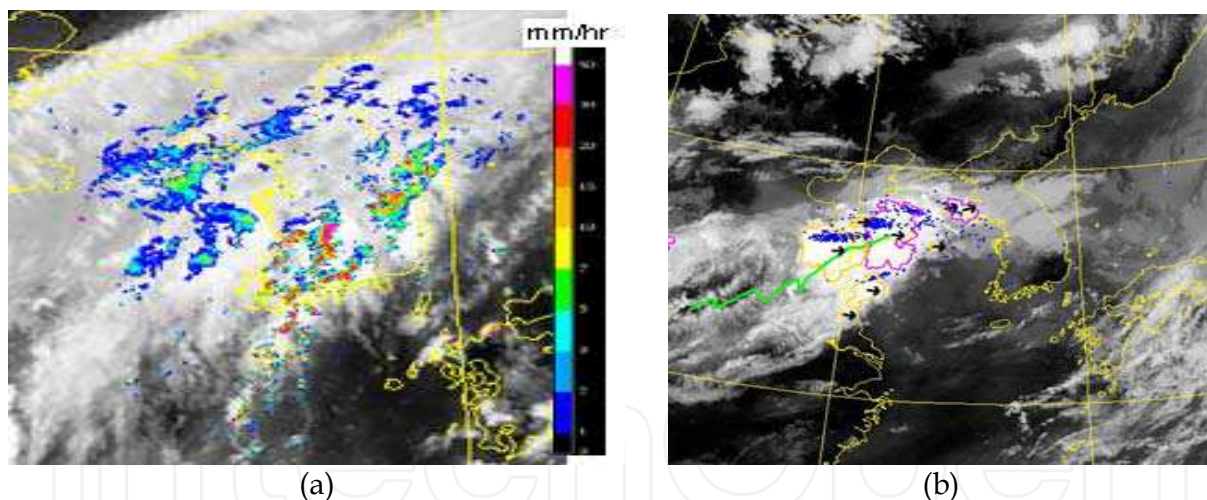


Fig. 27. Examples of COMS MI data applications (a) Convective rain intensity image combined with radar rain map (b) Predicted location of convective cloud and lightening image.

To analyze the Typhoon, which passes through Korean peninsula two to three times a year, typically around July to September time, such elements as the Typhoon intensity, radius of strong winds, the maximum wind speed, low pressure, are needed. In this analysis, NMSC is utilizing the Advanced Dvorak Technique (ADT) in the site operations, which was developed by the Cooperative Institute for Meteorological Satellite Studies (CIMSS) of University of Wisconsin (UW). The algorithm in this technique classifies the evolution phase of the tropical cyclone according to its intensity, as the formation phase, the development

phase and the disappearance phase, based on the MI infrared (IR) images, and automatically analyses the Typhoon intensity through the experience in pattern recognition by applying the Fast Fourier Transform (FFT) on the resulting patterns from the different phase of the cyclone.

COMS MI data are also to be used in the generation of aeronautical meteorological products, as shown in the Fig. 28. These products may have a relatively low accuracy but have the advantage of observing the broader area every hour. They are providing the level 2 information; such as the cloud phase, cloud height and the cloud top temperature in the air route and also the information from the convective cloud monitoring, and the other technique is under development for the information generation on the elements that can cause aircraft accidents, such as the icing and the turbulence.

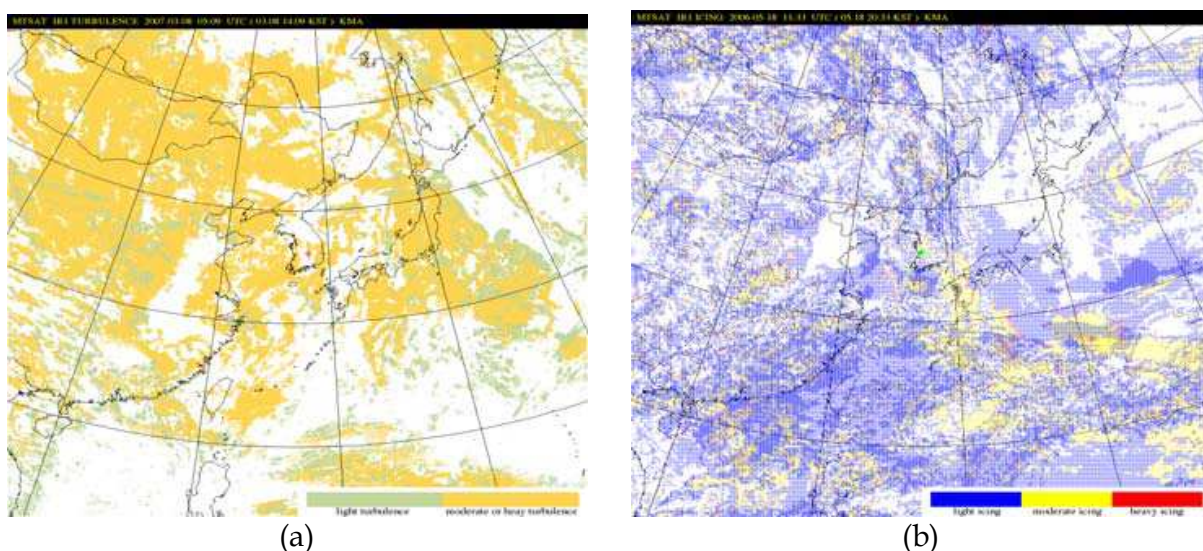


Fig. 28. Examples of COMS MI aeronautical meteorological products (under developments) (a) turbulence distribution (b) icing on airplane area .

4.2 GOCI

The application of GOCI data is focused on the monitoring of long-term/short-term ocean change phenomena around Korean peninsula and north-eastern Asian seas. In daytime, the hourly-produced GOCI data will be used for the ocean/coast environmental monitoring and for the observation of ocean dynamics features and the management of ocean territory. Also, these GOCI data, when used in conjunction with ocean numeric models, would bring forth the increase of accuracy in ocean forecasting.

GOCI level 2 data products can be generated from GOCI level 1B with GDPS (GOCI Data Processing System) which is the data processing and analysis software developed by KORDI.

This GDPS system derives the pure ocean signal (water leaving radiance) by atmospheric correction using aero-optics model and oceano-optics model developed and modified by KORDI. It can extract pure water signal as the normalized water leaving radiance which is corrected water leaving radiance by considering the satellite - sun relative geometry. For geostationary satellite, this relative position of the sun and the satellite changes all the time

and then the ocean signal is distorted. To resolve this issue of signal distortion, some research was performed. The system can generate the marine environment analysis data using specific algorithms for target region. The data processing algorithms applied to the existing ocean satellite optical sensor and new algorithms to the GOCI would produce the latest marine environmental analysis results.

Table 9 shows the list of GOCI level 2 data products which are currently being generated and used for each application purpose, and Table 10 signifies the list of GOCI level 3 data products which can also be generated by GDPS. The algorithm to generate GOCI level 3 data is under the final validation process. Fig. 29 shows some typical examples of these end products, in the case of TSS and CDOM.

| PRODUCTS | DESCRIPTION | APPLICATION |
|---|--|---|
| Water-leaving Radiance (Lw) | The radiance assumed to be measured at the very surface of the water under the atmosphere | Indispensible for water color analysis algorithms |
| Normalized water leaving radiance (nLw) | The water leaving radiance assumed to be measured at nadir, as if there was no atmosphere with the Sun at zenith | Input data for the water analysis algorithm |
| Chlorophyll (CHL) | Concentration of phytoplankton chlorophyll in ocean water | Ocean primary production estimation, dumping site monitoring, climate change monitoring |
| TSS | Total suspended sediment concentration in ocean water | Coastal ocean environmental analysis and monitoring TSS movement and transfer monitoring |
| CDOM | Colored dissolved organic matter concentration in ocean water | Indicator of ocean pollution Ocean salinity estimation |
| Optical properties of water | K-coefficient Absorption coefficient(a) Backscattering coefficient(bb) | Ocean optical properties analysis |
| Red tide (RI) | Red tide index information | Ocean pollution and ecological monitoring Movement and transfer monitoring of red tide |
| Underwater Visibility (VIS) | Degree of clarity of the ocean observed by the naked eye | Navy tactics, ocean pollution map, sea rescue work |
| Atm. & earth environment | Yellow dust, Vegetation Index | Atmospheric environment and land application |

Table 9. GOCI level 2 data products

| PRODUCTS | DESCRIPTION | APPLICATION |
|----------------------------------|---|--|
| Daily composite of CHL, SS, CDOM | Daily 8 images composite for cloud free mosaic image | Climate change trend analysis |
| Fishing ground Information (FGI) | Fishing ground probability index, fishing ground prediction | Fishing ground detection Fishing ground environmental information |

| PRODUCTS | DESCRIPTION | APPLICATION |
|----------------------------------|--|---|
| Sea surface current vector (WCV) | Sea surface current direction/speed | Understanding of sea surface currents and estimation of pollutant movements |
| Water quality Level (WQL) | Coastal water quality level estimation | Coastal ocean eutrophication Coastal water quality control/monitoring |
| Primary Productivity (PP) | The production of Organic compounds from carbon dioxide, principally through the process of photosynthesis | Carbon cycle Long-term climate change monitoring |

Table 10. GOCI level 3 data products

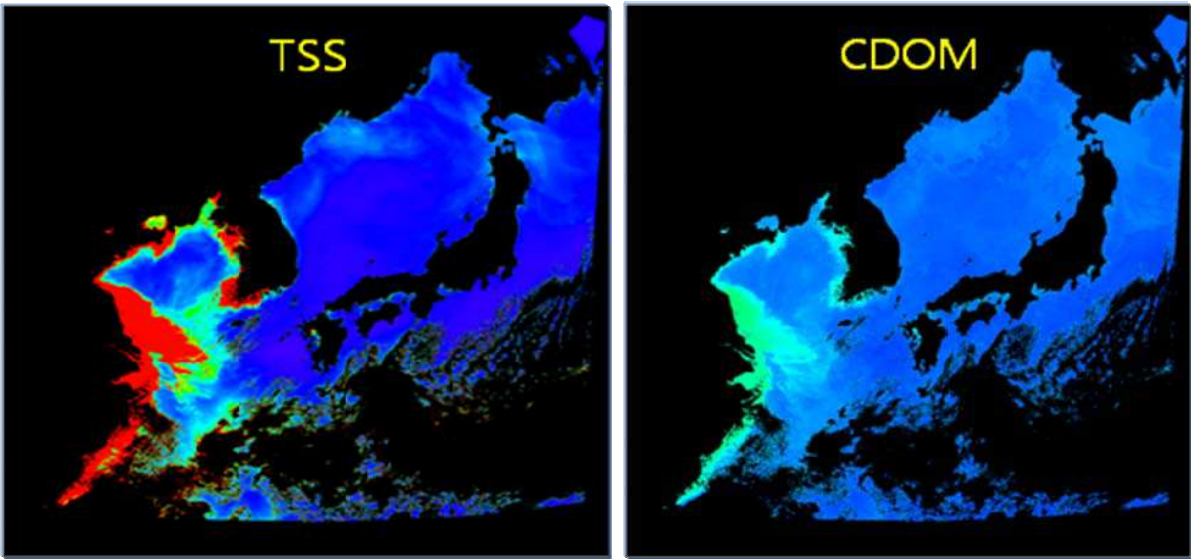


Fig. 29. Examples of GOCI level 2 end products, TSS (Total Suspended Sediment) and CDOM (Colored Dissolved Organic Matter)

GOCI products such as ocean current vector and ocean color properties would be provided to the fishery and the related organization for the increase of the haul, the effective management of fish, and finally the increase of fisheries income. The GOCI data could also be useful for monitoring suspended sediment movement, pollution particles movement, ocean current circulation and ocean ecosystem. Also, it will contribute to the international cooperation system, such as GEOSS (Global Earth Observation System of Systems), for the long-term ocean climate change related research and application by the data exchange and co-research among related countries.

The Korea Ocean Satellite Center (KOSC) in KORDI as the official GOCI operation agency, receives the GOCI data from the satellite directly, generates, stores, manages and distributes the processed standard products. And KOSC will continuously develop new ocean environmental analysis algorithms to apply to the imagery data of GOCI and the GOCI-II which is next generation of GOCI.

Through the normal operation of GOCI, KOSC can provide the new, high-grade ocean environmental information in near-real time. It can be applied to the detection of freak phenomena of ocean nature such as the red-tide and the green-tide. The primary

productivity derived from the GOCI chlorophyll and other products is the key research information about ocean carbon circulation. The color RGB images and analysis images of GOCI products with high spatial resolution are clearer and more recognizable than the monochrome images from other existing geostationary earth monitoring satellite which has only 1 visible band. These images can be useful to land application and atmospheric remote sensing application like monitoring of typhoon, sea ice, forest fire, yellow dust, etc.

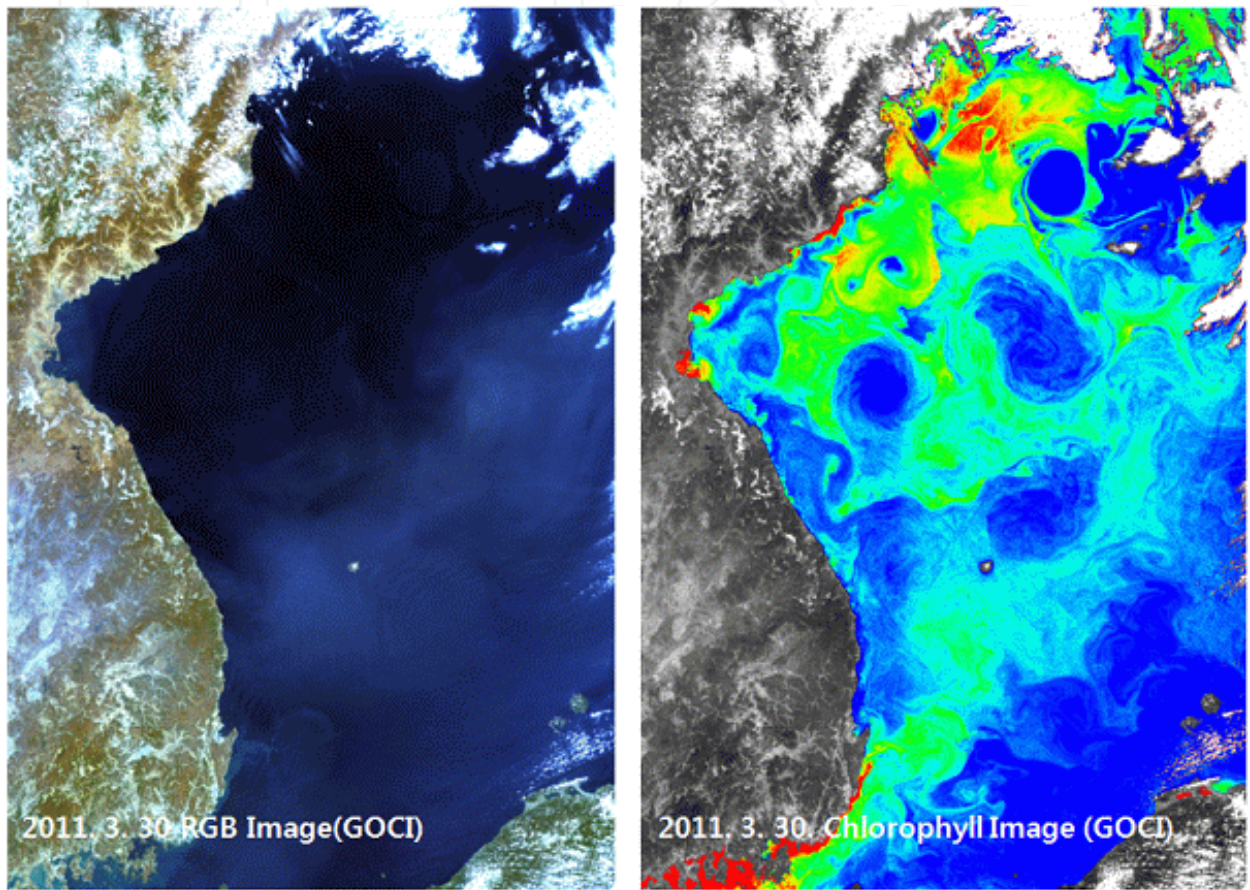


Fig. 30. Standard RGB image of GOCI (left) and the analysis result of seawater chlorophyll density in the East Sea (right)

Table 11 shows the overall scheme of GOCI data application, and Fig. 31 and Fig. 32 exemplify some of the typical applications. In Fig. 32, several Images of different dates were mosaiced to realize this cloud-free picture and the numerical signals of the Yellow Sea (East China Sea), the East Sea (Japan Sea) and Northwestern Pacific were differently processed to maintain a balanced tone throughout the whole coverage area of the GOCI.

| Operation | Application Items |
|-------------------------------|---|
| Carbon Circulation Monitoring | <div>- Analysis of marine primary productivity</div> <div>- Long-term climate change research in the ocean</div> <div>- Long-term analysis of climate change through research studies and utilized to secure carbon credits</div> |

| Operation | Application Items |
|--|--|
| Red Tide Monitoring | - Amounts of red tide, forecast to move through the path and spread of red tide-related damage contribute to the reduction |
| Green Algae Monitoring | - Amounts of green algae, forecast to move through the path and spread of green algae-related damage contribute to the reduction |
| Oil spill monitoring | - Oil spill and monitoring of movement and distribution of pollution |
| Speculative waters, environmental monitoring | - Ocean dumping in the waters of chlorophyll contained in phytoplankton concentration and monitoring the amount of organic matter dissolved in seawater |
| Turbidity Monitoring | - Indicators of marine pollution - The total suspended inorganic material contained in seawater through the coastal marine environment observation analysis and monitoring |
| Low-salinity water monitoring | - Utilization of seawater salinity estimates (Low-salted water monitoring) - Which flows from China to determine the utilization of contaminant migration path |
| Fishery Information | - Fish and Fishery distribution - Fisheries and environmental monitoring and fisheries contribute to productivity improvement |
| Fisheries and fish-farm management | - Long-term monitoring of marine ecosystems through the efficient management of fisheries resources |
| Ecological monitoring tidal | - Marine Biology / Ecological Survey, appeal / river forecasts, and productivity of aquatic organisms in the environment - Coastal fisheries resources management |
| Hurricane watch | - A hurricane tracking and navigation path - The impact of Hurricane directed by the ocean, producing flow information |
| Sea-ice monitoring | - Development of the area of sea ice observations and monitoring - Support fishing operations |
| Forest fire monitoring | - land management and forest fire monitoring, forest resources utilization |
| Dust monitoring | - Dust, vegetation, and the atmosphere and global environmental monitoring information - Dust weather analysis and forecasting, and utilized in the atmospheric environment |
| Current surveillance | - Balm of seawater, and the flow rate information production - Utilize coastal water quality management |
| El Niño, La Niña monitoring | - Estimated using ocean temperature and productivity monitoring long-term climate change |

Table 11. Application subjects of GOCI data

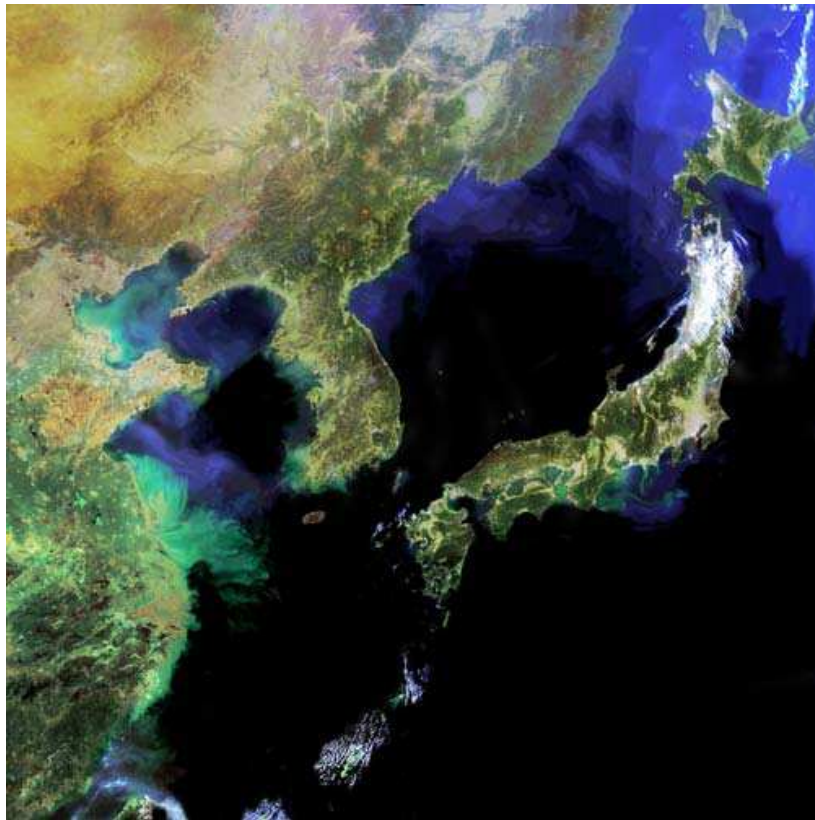


Fig. 31. Land and Sea Features expressed by natural color on the full scene of the GOCI.

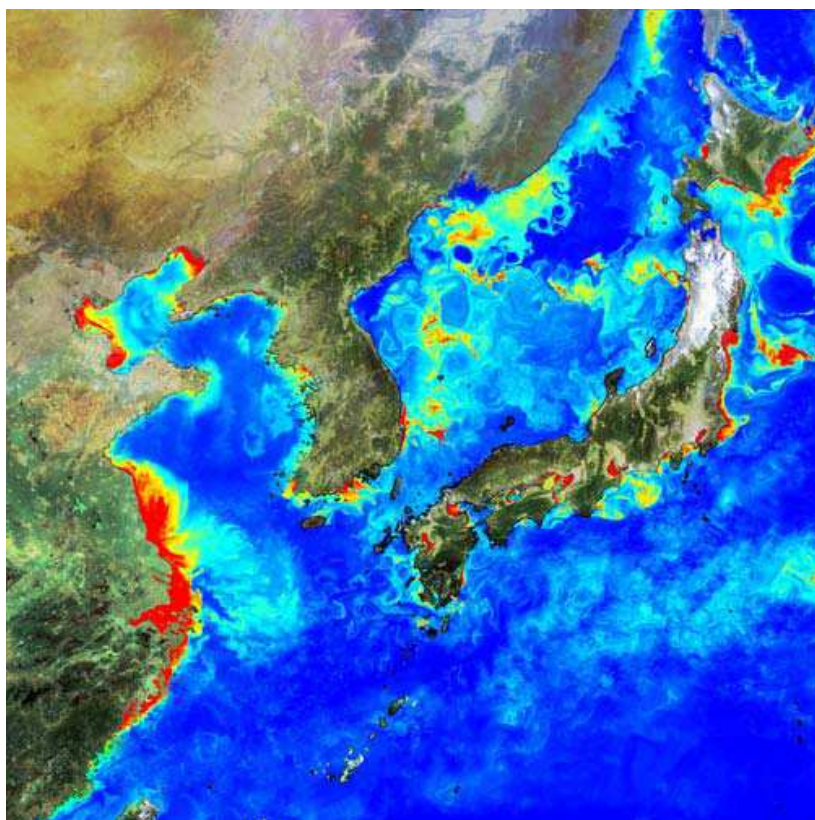


Fig. 32. Structure of Chlorophyll Distribution in the North-East Asian Seas.

5. Conclusion

COMS is a unique bird in many ways, partially in that it is such a complex satellite accommodating three different payloads with rather conflicting missions into a single spacecraft bus, partially in that it employs a unique and novel INR system, and also partially because it has the GOCI on board, the world's 1st geostationary imager for the ocean colour. By the joint effort of EADS Astrium and KARI, it was masterfully designed, developed, tested, and launched, and is now behaving beautifully in orbit, exhibiting quite impressive and fruitful performances along with the very useful and interesting image data and processed end products.

It is especially interesting to note that with the co-existence of both MI and GOCI on board, the comparison and combination of data taken by these two sensors from the same geostationary location, could open some new windows for further interesting research and development. In the case of GOCI, the benefits of Geo observation compared to its LEO (Low Earth Orbit) counterparts has been notably demonstrated and largely appreciated by the end users so far, even with the relatively short accumulated time of normal service, and as the further activities on post processing and related studies will get refined and matured, it is expected that this trend will become even more prominent.

With these observations, findings and expectations at hand, it could be cautiously said that COMS image data and the processed end products will bring some added dimension to the world remote sensing community and the related field of science and technology. For this end, it will be made sure that the application of MI and GOCI data during the mission life of COMS is to be fully exploited and maximized. It is hoped and believed that all the aspects of the COMS development and operation; from the design, implementation, test and validation, launch and IOT, to the data processing, end product generation, data utilization and end user services will continue to grow and be improved and expanded in its relevant realm into the next generation of geostationary remote sensing satellites.

6. Acknowledgment

COMS program has involved so many different organizations, agencies, government bureaus and companies and wide spectrum of participating personnel with different cultures, characters and backgrounds. It is with such a great emotion and gratitude, along with the highly rewarding feeling and sense of proud accomplishment, that we can now say that we regard all the participating members in this program as one big 'COMS family' and to some, very close life-long friends, indeed. There were certainly some bumpy roads and rocky times in the course, but through them all we became real friends and it is grateful that we can now look back upon those days with sense of mutual respect and appreciation.

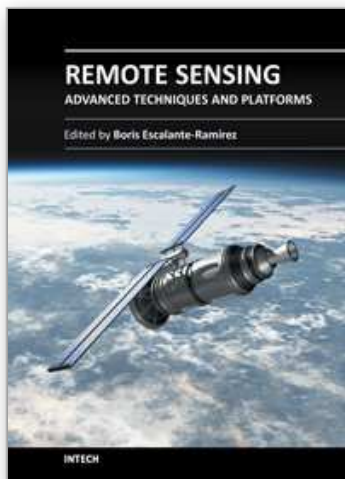
We feel deeply grateful and obliged to send our appreciation to our Korean government bureaus first and foremost; MEST (Ministry of Education, Science and Technology), KMA (Korea Meteorological Administration), KORDI (Korea Ocean Research & Development Institute), MLTM (Ministry of Land, Transport and Maritime Affairs) and MIC (Ministry of Information and Communication), among others, without whose support and dedication this grand program would not have been possible. We feel especially thankful to MOSF (Ministry Of Strategy and Finance) for providing us the actual revenue sources continually throughout the entire course of this challenging program.

The author and co-authors of this chapter only represent a very small portion of all COMS family members, and we believe that the authors of this chapter, in fact, ought to be all COMS family members and thus we feel deeply indebted to them. Our special thanks go to; Mr. Seong-rae Jung and Ms. Jin Woo of KMA, and Mr. Hee-jeong Han and Mr. Seong-ik Cho of KORDI, for the charts in the section 3.3.2 and for their great help and support in preparing and finalizing sections 4.1 and 4.2.

Last but clearly not the least, we remember our missing COMS family members, Mr. Daniel Buvat of EADS Astrium and Mr. Young-joon Chang and Mr. Sang-mu Moon of KARI, who abruptly departed from this life on earth in the course of COMS development and operation, leaving the rest of us in deep grief and helpless devastation. Along the lines of COMS history, with the trace of their sincere commitment and contribution to the success of COMS, they will always be remembered in our hearts. We dedicate this small chapter to them.

7. References

- Cros, G.; Loubières, P.; Lainé, I.; Ferrand, S.; Buret, T.; Guay, P. (June 2011) *European ASTRIX FOGS In-Orbit Heritage*, 8th International ESA Conference on Guidance, Navigation & Control Systems
- Kang, G.; Coste, P. (2010) *An In-orbit Radiometric Calibration Method of the Geostationary Ocean Color Imager (GOCI)*, IEEE Transactions on Geoscience and Remote Sensing, Digital Object Identifier 10.1109 / TGRS. 2010. 2050329
- Kim, H.; Kang, G.; Ellis, B.; Nam, M.; Youn, H.; Faure, F.; Coste, P.; Servin, P. (2009) *Geostationary Ocean Color Imager (GOCI), Overview and Prospect*, 60th International Astronautical Congress (IAC 2009)
- Kim, H.; Meyer, P.; Crombez, V.; Harris, J. (2010) *COMS INR: Prospect and Retrospect*, 61st International Astronautical Congress (IAC 2010)
- Lambert, H.; Koeck, C.; Kim, H.; Degremont, J.; Laine, I. (2011) *One Year into the Success of the COMS Mission*, 62nd International Astronautical Congress (IAC 2011)
- KARI (Korea Aerospace Research Institute) (January 2006). *COMS Ground Segment Specification, Ref C1-SP-800-001-Rev.C*, Deajeon, KOREA
- Lee, B.; Jeong, W.; Lee, S.; et al. (April 2006). *Functional Design of COMS Satellite Ground Control System*, Conference of the Korean society for aeronautical and space science, pp. 1000-1005, KSAS06-1850.
- Lim, H.; Ahn, S.; Seo, S.; Park, D. (December 2011). *In-Orbit Test Operational Validation of the COMS Image Data Acquisition and Control System*, Journal of the Korean society of Space Tehnology, Vol.6 No.2, pp. 1- 9.



Remote Sensing - Advanced Techniques and Platforms

Edited by Dr. Boris Escalante

ISBN 978-953-51-0652-4

Hard cover, 462 pages

Publisher InTech

Published online 13, June, 2012

Published in print edition June, 2012

This dual conception of remote sensing brought us to the idea of preparing two different books; in addition to the first book which displays recent advances in remote sensing applications, this book is devoted to new techniques for data processing, sensors and platforms. We do not intend this book to cover all aspects of remote sensing techniques and platforms, since it would be an impossible task for a single volume. Instead, we have collected a number of high-quality, original and representative contributions in those areas.

How to reference

In order to correctly reference this scholarly work, feel free to copy and paste the following:

Han-Dol Kim, Gm-Sil Kang, Do-Kyung Lee, Kyoung-Wook Jin, Seok-Bae Seo, Hyun-Jong Oh, Joo-Hyung Ryu, Herve Lambert, Ivan Laine, Philippe Meyer, Pierre Coste and Jean-Louis Duquesne (2012). COMS, the New Eyes in the Sky for Geostationary Remote Sensing, Remote Sensing - Advanced Techniques and Platforms, Dr. Boris Escalante (Ed.), ISBN: 978-953-51-0652-4, InTech, Available from:
<http://www.intechopen.com/books/remote-sensing-advanced-techniques-and-platforms/coms-the-new-eyes-in-the-sky-for-geostationary-remote-sensing>

INTECH
open science | open minds

InTech Europe

University Campus STeP Ri
Slavka Krautzeka 83/A
51000 Rijeka, Croatia
Phone: +385 (51) 770 447
Fax: +385 (51) 686 166
www.intechopen.com

InTech China

Unit 405, Office Block, Hotel Equatorial Shanghai
No.65, Yan An Road (West), Shanghai, 200040, China
中国上海市延安西路65号上海国际贵都大饭店办公楼405单元
Phone: +86-21-62489820
Fax: +86-21-62489821

© 2012 The Author(s). Licensee IntechOpen. This is an open access article distributed under the terms of the [Creative Commons Attribution 3.0 License](https://creativecommons.org/licenses/by/3.0/), which permits unrestricted use, distribution, and reproduction in any medium, provided the original work is properly cited.

IntechOpen

IntechOpen